

Report No. RD-64-156

AD611444

## FINAL REPORT

Project No. 320-205-02X

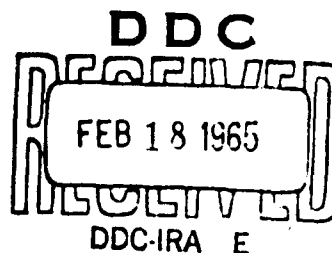
# TEST OF TRAIL CONE SYSTEM TO CALIBRATE STATIC PORTS FOR BAROMETRIC ALTIMETERS



COPY	2	OF	3	only
HARD COPY	\$ .300			
MICROFICHE	\$ .075			

65 P

DECEMBER 1964



**FEDERAL AVIATION AGENCY**  
Systems Research & Development Service  
Atlantic City, New Jersey

REPRODUCED FROM  
BEST AVAILABLE COPY

ARCHIVE COPY

FINAL REPORT

TEST OF TRAIL CONE SYSTEM TO CALIBRATE  
STATIC PORTS FOR BAROMETRIC ALTIMETERS

PROJECT NO. 320-205-02X

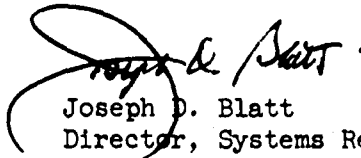
REPORT NO. RD-64-156

Prepared by:

Jack J. Shrager

December 1964

This report has been approved for general availability. It does not necessarily reflect FAA policy in all respects and it does not, in itself, constitute a standard, specification or regulation.



Joseph D. Blatt  
Director, Systems Research  
and Development Service  
Federal Aviation Agency

Experimentation Division  
National Aviation Facilities Experimental Center  
Atlantic City, New Jersey

REPRODUCED FROM  
BEST AVAILABLE COPY

## TABLE OF CONTENTS

	Page
ABSTRACT.....	1v
INTRODUCTION .....	1
TRAILING CONE SYSTEM DESCRIPTION .....	2
TEST PROCEDURES .....	9
Phototheodolite/Atmospheric Observation .....	9
Vertical Aerial Camera/Atmospheric Observation .....	11
Tower Fly-By .....	14
Radar Tracking/Pressure Survey .....	14
Radar Phototheodolite/Radiosonde .....	14
Pacer/Chase .....	18
Temperature Profile Survey .....	18
Density Profile Survey .....	18
TEST EQUIPMENT .....	18
TV-2 Pacer Aircraft .....	18
F8C Pacer Aircraft .....	23
Ground Base Equipment .....	25
METHOD OF ANALYSIS .....	29
TEST RESULTS AND ANALYSIS .....	39
CONCLUSIONS .....	55
RECOMMENDATIONS .....	55
LIST OF SYMBOLS .....	56
REFERENCES.....	57

# LIST OF ILLUSTRATIONS

Figure		Page
1	British High-Speed Pitot Static Tube .....	3
2	Aircraft Trailing High-Speed Tube .....	4
3	Douglas Cone Assembly .....	5
4	NAFEC Cone Assembly .....	6
5	Reel Assembly .....	7
6	Cone in Flight Behind Aircraft .....	8
7	Drag Curve for Standard Cone .....	10
8	Aircraft Flight Path - Field Layout .....	12
9	Aircraft Flight Path Over Vertical Camera .....	13
10	Aircraft Flight Path for Tower Fly-By .....	15
11	Pressure Survey at Altitude .....	16
12	Aircraft Overtake Method .....	18
13	Flight Pattern at Varying Airspeeds and Constant Altitude .....	19
14	TV-2 Test Aircraft .....	20
15	Photopanel of TV-2 .....	22
16	F8C Test Aircraft .....	24
17	Photopanel of F8C .....	26
18	Phototheodolite System .....	27
19	Aerial Camera .....	28
20	X-Band Radar (TARE) .....	30

# LIST OF ILLUSTRATIONS (continued)

Figure		Page
21	Radiosonde .....	31
22	Barometer .....	32
23	Psychron Unit .....	33
24	Position Error Versus Indicated Airspeed - TV-2 Pacer (Low Altitude) All Data .....	42
25	Position Error Versus Indicated Airspeed - TV-2 Pacer (Low Altitude) Selected Data .....	43
26	Position Error Versus Indicated Airspeed - F8C Pacer (Low Altitude) All Data .....	44
27	Position Error Versus Indicated Airspeed - F8C Pacer (Low Altitude) Selected Data .....	45
28	Position Error Versus Indicated Airspeed - F8C Pacer (High Altitude) All Data .....	46
29	Position Error Versus Indicated Airspeed - F8C (High Altitude) Selected Data .....	48
30	Position Error Versus Indicated Airspeed - All Selected Data .....	49
31	$\Delta P/q_C$ Versus $M_n$ (TV-2 Pacer) .....	50
32	$\Delta P/q_C$ Versus $M_n$ -F8C Pacer (Low Altitude) .....	51
33	$\Delta P/q_C$ Versus $M_n$ -F8C Pacer (High Altitude) .....	52
34	$\Delta P/q_C$ Versus $M_n$ -All Data .....	53
35	$\Delta H$ Versus IAS-All Data .....	54

Federal Aviation Agency, Systems Research and Development Service,  
National Aviation Facilities Experimental Center, Experimentation  
Division, Atlantic City, N. J.

TEST OF TRAIL CONE SYSTEM TO CALIBRATE STATIC PORTS FOR BAROMETRIC  
ALTIMETERS by Jack J. Shrager, Final Report, December 1964, 59 pp.  
incl. 35 illus.

(Project No. 320-205-02X, Report No. RD-64-156)

#### ABSTRACT

An experimental trail cone stabilized static source system was fabricated and tested using various towing aircraft at speeds up to 1.12 Mach Number to determine its suitability as a "standard" method for determining altimeter static pressure error. Flight tests were conducted at sea level, 5,000, 10,000, 15,000, 25,000, 30,000 and 40,000 feet, to determine the static pressure defect of the trailing cone system. Test results indicated that the experimental system had a nominal "position error" equal to + 12 feet at sea level and + 30 feet at 30,000 feet.

## INTRODUCTION

The pilot of an aircraft determines his flight altitude by referring to the aircraft's barometric pressure altimeter. Since the instrument's presentation is a function of the "sensed" ambient pressure, it is necessary to know the difference between sensed and true ambient pressure to determine actual pressure altitude. This difference, generally referred to as "position error," is affected by many factors including (a) type of the aircraft's static pressure probe, (b) location of the static pressure probe, (c) angle of attack of the aircraft, and (d) flight speed of the aircraft as related to the velocity of sound, Mach Number (Mn).

There are several methods currently employed to determine the position error. The magnitude of the position error at flight altitudes below 1000 feet up to the limit of the operational characteristics of the aircraft can readily be determined. There are several theoretical procedures for extrapolating low-altitude results to cover the entire operational envelope of the aircraft but even these procedures include certain assumptions not readily verified.

The purpose of this Federal Aviation Agency's (FAA) Research and Development Project was to develop, if possible, or define an acceptable standard for determining the position error. This method is to be usable for general aviation, commercial carrier aircraft, and military aircraft at all applicable altitudes and throughout all flight speeds including subsonic, transonic, and supersonic velocities.

A secondary, though not necessarily restrictive, consideration is to evolve an economically feasible system which could be readily implemented by the aviation industry. This secondary consideration is not to be restrictive on the desired attainable accuracy which is to be that within the capability of the best known selected flight instruments with special precision calibration.

A review of all known published information, Reference A to C, was made to determine the theoretical requirements and the possible design specifications of a system which would meet the desired requirements. This report covers the test procedures and results for such a proposed system; namely, a trailing cone stabilized static pressure source. This system is based on a refinement of technique originally suggested by the Royal Aeronautical Society, Reference AH, modified by the Douglas Aircraft Company, Reference B, and further modified by the FAA to meet the requirements noted above.

The results contained in this report include those obtained at the FAA's National Aviation Facility Experimental Center (NAFEC), and the Naval Air Test Center (NATC) in cooperation with the Bureau of Weapons, U. S. Navy.

#### TRAILING CONE SYSTEM DESCRIPTION

The cone stabilized static source is an outgrowth of a Royal Aircraft Establishment method using a high-speed Pitot static tube, Fig. 1, which was attached to a flexible, hollow molybdenum steel tube that trailed behind and below the aircraft under test, as shown in Fig. 2.

The Douglas Aircraft Company's version of this system utilized a fiberglass cone to stabilize the tube assembly with the static holes drilled in the tubing itself. The final Douglas version used nylon tubing in place of the flexible steel tubing, Fig. 3.

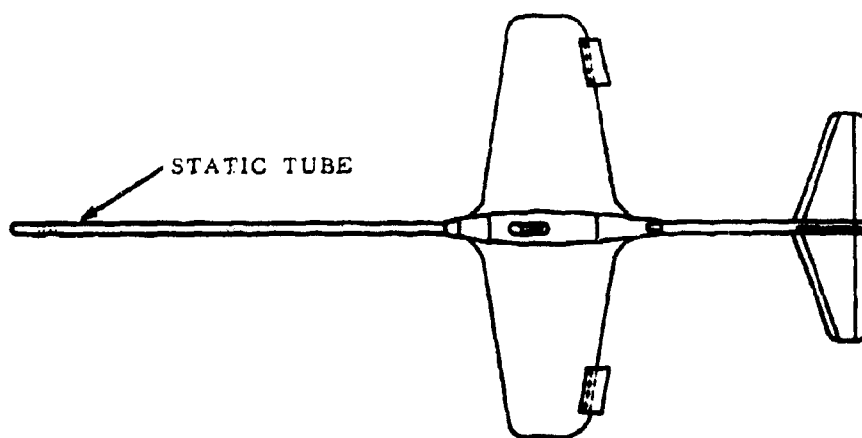
The FAA's experimental system built by Douglas Aircraft Company to FAA specifications utilized a stainless steel insert containing the static ports approximately 10 feet forward of the fiberglass cone. A stainless steel wire was inserted throughout the length of the assembly to carry the drag force, thus preventing separation of the nylon tubing from the metal insert. The system was later modified to permit free rotation of the cone without introducing a torsional moment to the wire insert. The system in its final configuration, as modified by NAFEC, is shown in Fig. 4.

All of the above noted systems utilized a reel and drive motor assembly which was installed in the test aircraft to extend and retract the drag body and hollow tube behind the aircraft. A typical reel assembly is presented in Fig. 5.

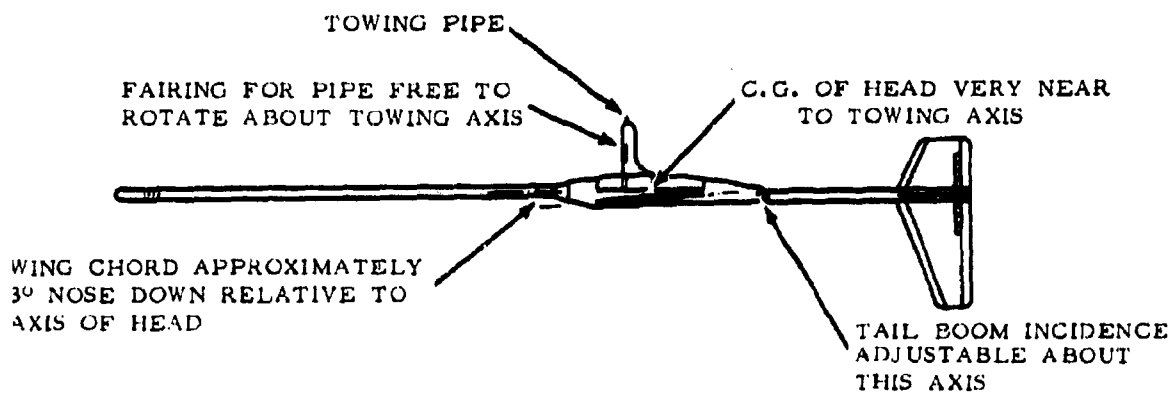
All systems in which the fiberglass cone was employed resulted in the tube assembly trailing in line with the attachment point of the aircraft, as shown in Fig. 6, instead of below the aircraft, Fig. 2, with the high-speed Pitot tube.

The total flow area of the static ports in the steel tube insert and in the drive reel mechanism was equal to or greater than the flow area of the plastic tube with the support wire inserted. The holes were located in a manner which would minimize any angle-of-attack effect of the steel tube insert.





PLAN VIEW



SIDE ELEVATION

FIG. 1 BRITISH HIGH-SPEED PITOT STATIC TUBE

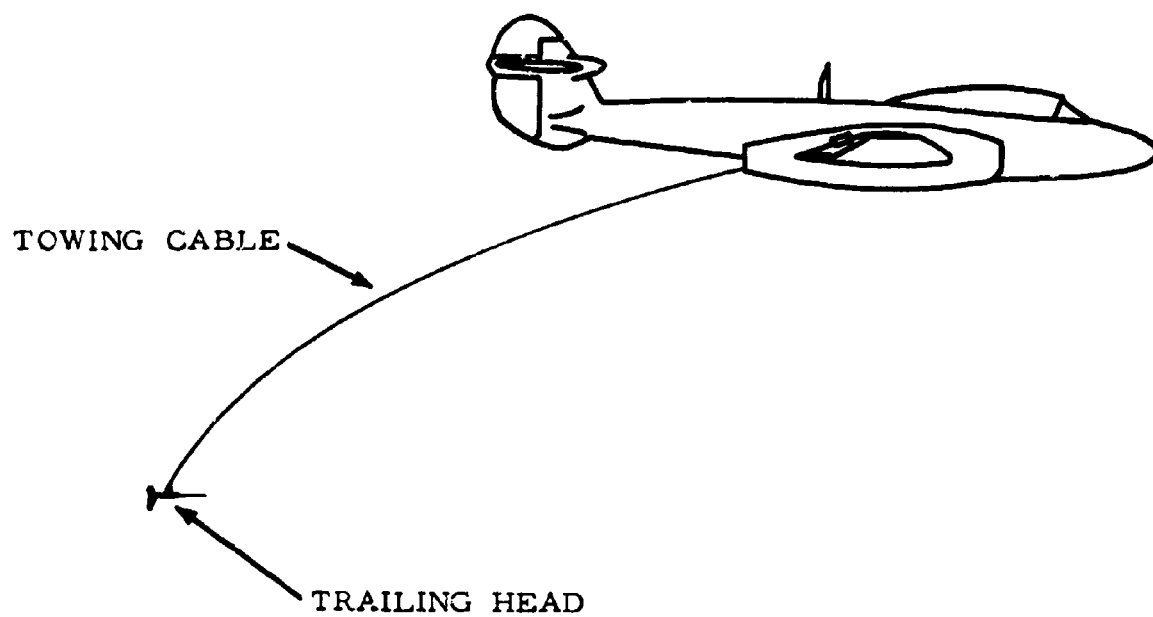
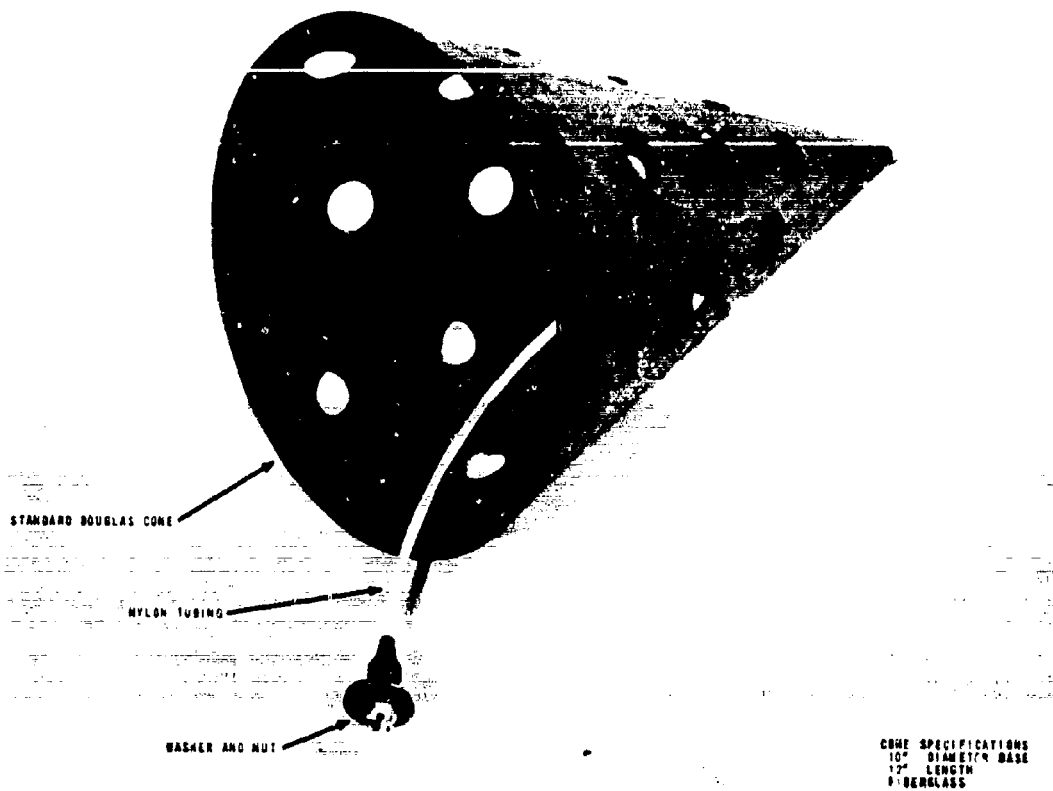
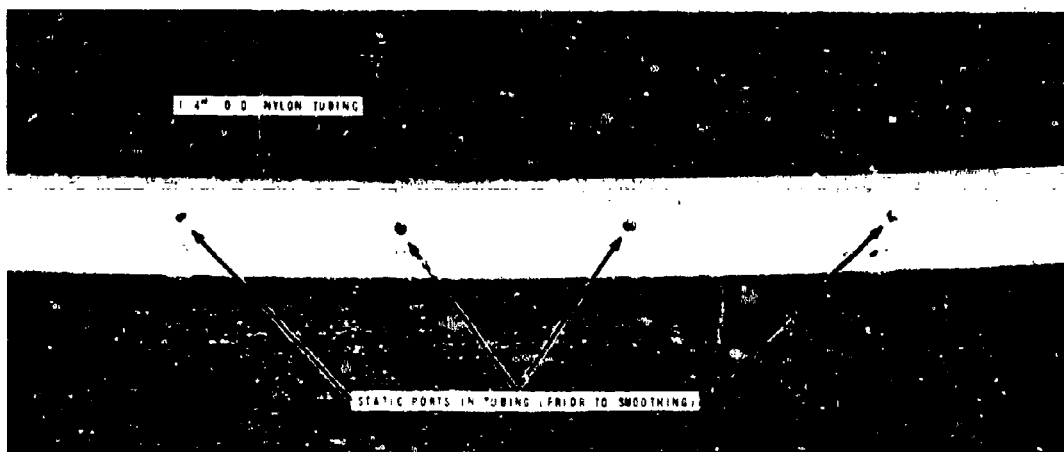


FIG. 2 AIRCRAFT TRAILING HIGH-SPEED TUBE

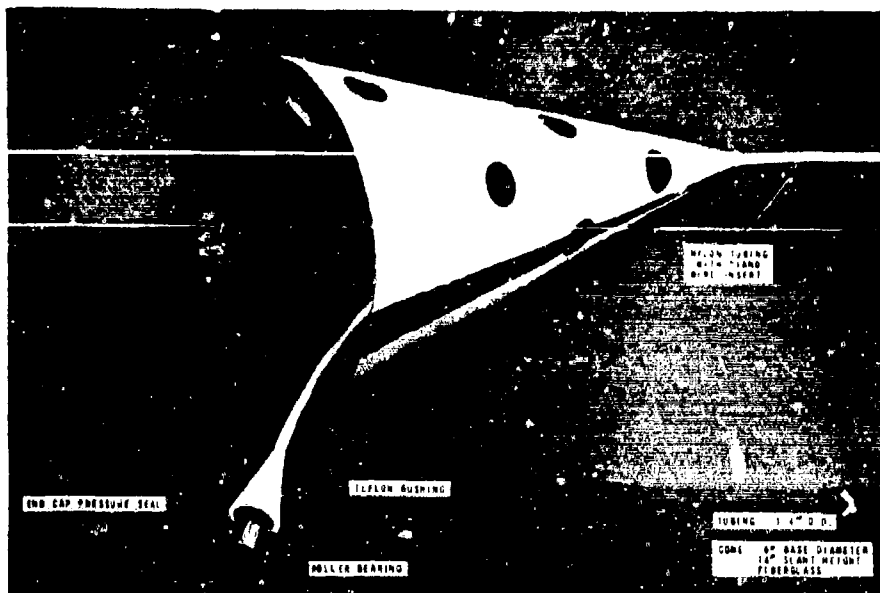


a. DOUGLAS CONE

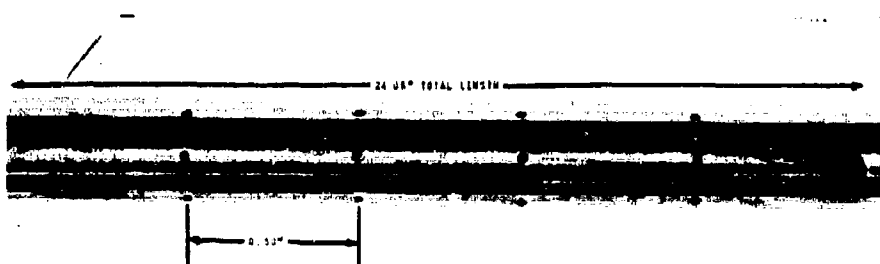


b. NYLON TUBING

FIG. 3 DOUGLAS CONE ASSEMBLY



a. NAFEC CONE



TUBE: 0.75\"/>

b. STEEL INSERT



c. OVERALL ASSEMBLY

FIG. 4 NAFEC CONE ASSEMBLY

FIG. 5 REEL ASSEMBLY

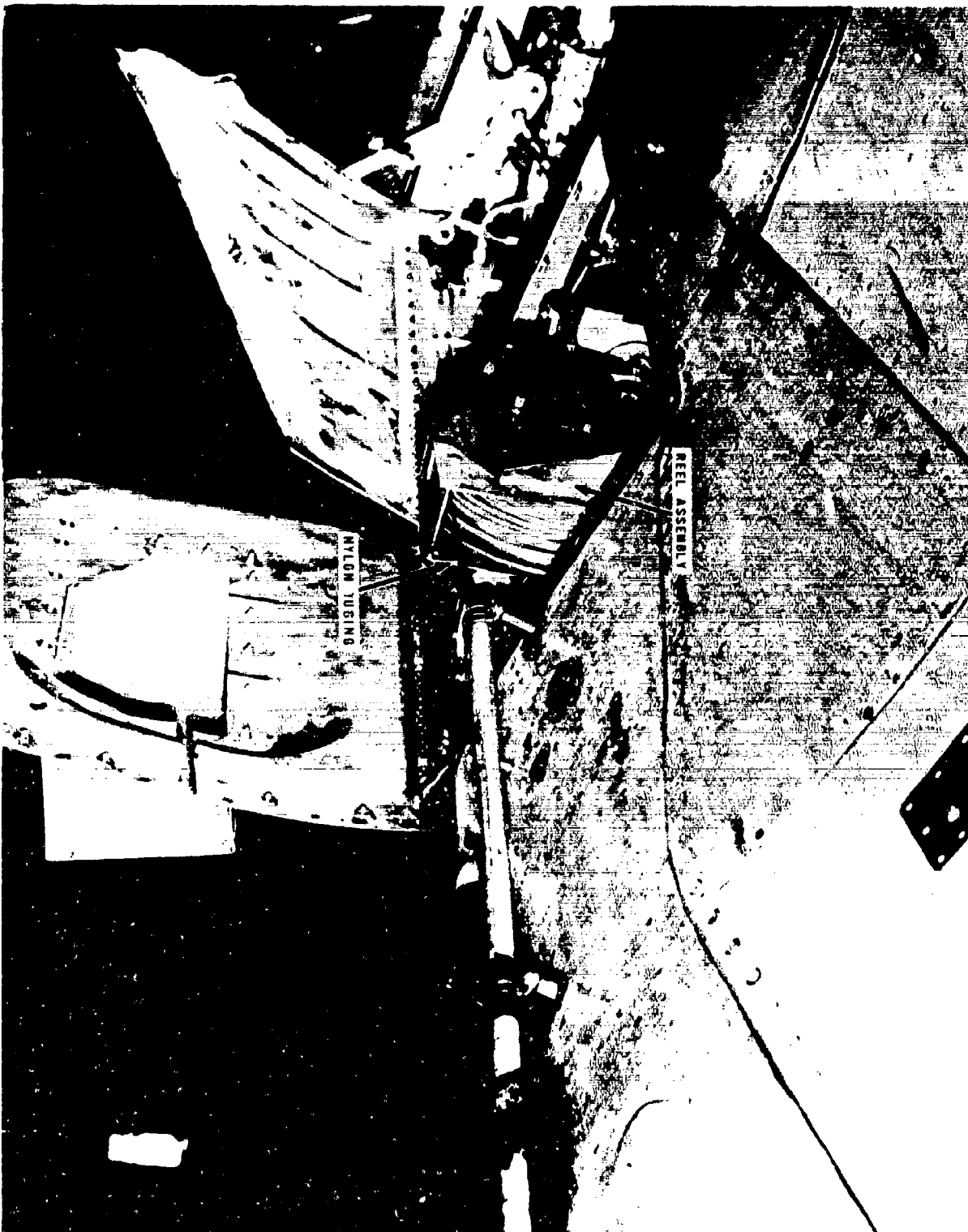
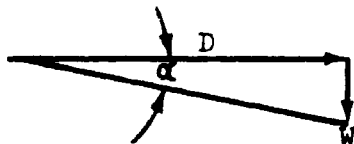


FIG. 5 REEL ASSEMBLY



FIG. 6 CONE IN FLIGHT BEHIND AIRCRAFT

The drag forces of the cone assembly, Fig. 7, were so great with respect to the mass of the complete tubing and cone assembly that the change in the angle of attack of the tube could be considered to be constant and approaching zero. This can be seen in the sample problems below at a nominal sea-level velocity of 160 knots, 0.24 Mn ( $q_c = 0.940$  inch Hg.) and 450 knots, 0.75 Mn ( $q_c = 8.00$  inches Hg.)



W=cone assembly weight=0.3 pounds

W=cone assembly weight=0.3 pounds

D=Drag Force at 160 knots=17 pounds

D=Drag Force at 450 knots=148 pounds

$$\tan \alpha = \frac{0.3}{17} = 0.01765$$

$$\tan \alpha = \frac{0.3}{148} = 0.00203$$

$$\alpha = 1.01^\circ$$

$$\alpha = 0.12^\circ$$

The system may be considered as the rigid nose boom of the fiberglass cone with an angle of attack equal to the angle of attack of the symmetrical conical body. The static ports, located forward of the cone by approximately 10 times the effective body size, should result in a pressure ratio error approaching zero, up through 1.02 Mn as noted in References L and AA.

#### TEST PROCEDURES

The test procedures employed to determine the position error of the trailing cone system were, as listed below, based on the physical resources available or their limitation under the conditions as employed. For report reference purposes only, they are further identified by sequential Roman numerals.

##### I. Phototherodolite/Atmospheric Observation

Prior to takeoff, all instruments both airborne and ground-located were read and recorded. When available, a radiosondic survey of the atmosphere up to the maximum test altitude was also made.

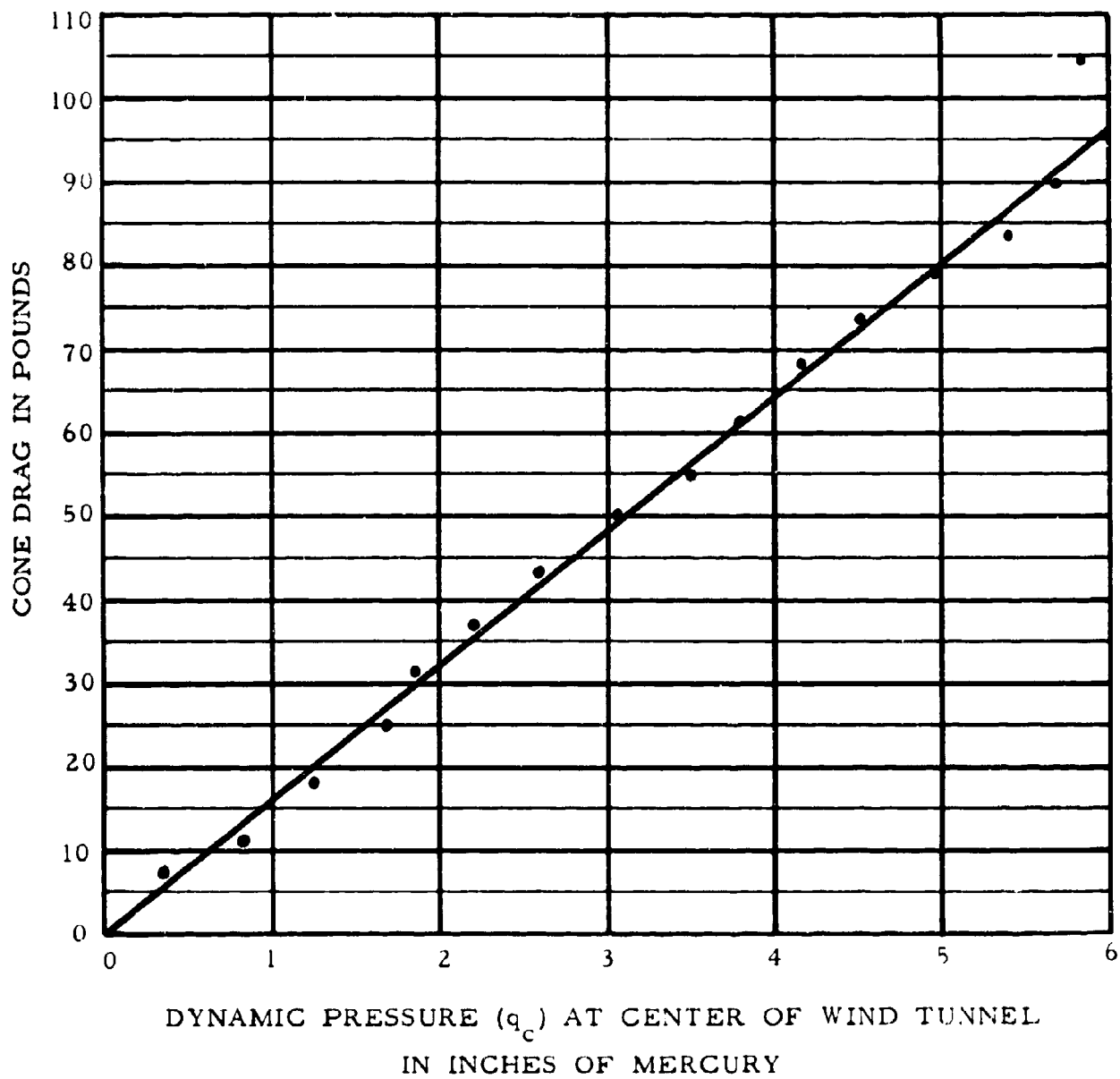


FIG. 7 DRAG CURVE FOR STANDARD CONE



After takeoff, the aircraft was flown in non accelerating level flight at both 0.55 Mn and the minimum indicated airspeed applicable for maximum gross weight in the aircraft's cruise configuration. Each test point, which was repeated twice, was made at an altitude of less than 500 feet above the nominal runway elevation.

At the completion of these reference speed points, the aircraft was flown in non accelerating level flight at various airspeeds from minimum controllable to maximum continuous or maximum allowable, whichever was greater, at low altitude (less than 500 feet above mean airport elevation), 5,000- and 10,000- foot altitudes in close proximity to NAFEC. Both airborne and ground recordings were taken at each test point from runway threshold to the end of the runway. The aircraft's flight path, Fig. 8, was designed to permit computation of airspeed from ground tracking information and to allow for stabilization of the aircraft prior to crossing the runway threshold.

The last data points for any flight were a repetition of the reference speed points, 0.55 Mn and minimum indicated airspeed cruise configuration. The aircraft would then land, taxi to the point where the original ground readings were made, and all instruments would be read and recorded. In addition, a radiosondic survey of the atmosphere would be repeated.

## II. Vertical Aerial Camera/Atmospheric Observation

The test procedure employed was similar to that described in Test Procedure I with the following noted exceptions:

The aircraft's flight path, Fig. 9, was directed over a high-precision aerial camera. At the instant the aircraft was directly overhead, a photograph of the aircraft was taken. This procedure, which is a modification of the tower fly-by method, is outlined in detail in Reference AC.

This method as well as the tower fly-by method described in Test Procedure III is used only for tests at low altitude (less than 1,000 feet above camera elevation).

FIG. 9 AIRCRAFT FLIGHT PATH OVER VERTICAL CAMERA

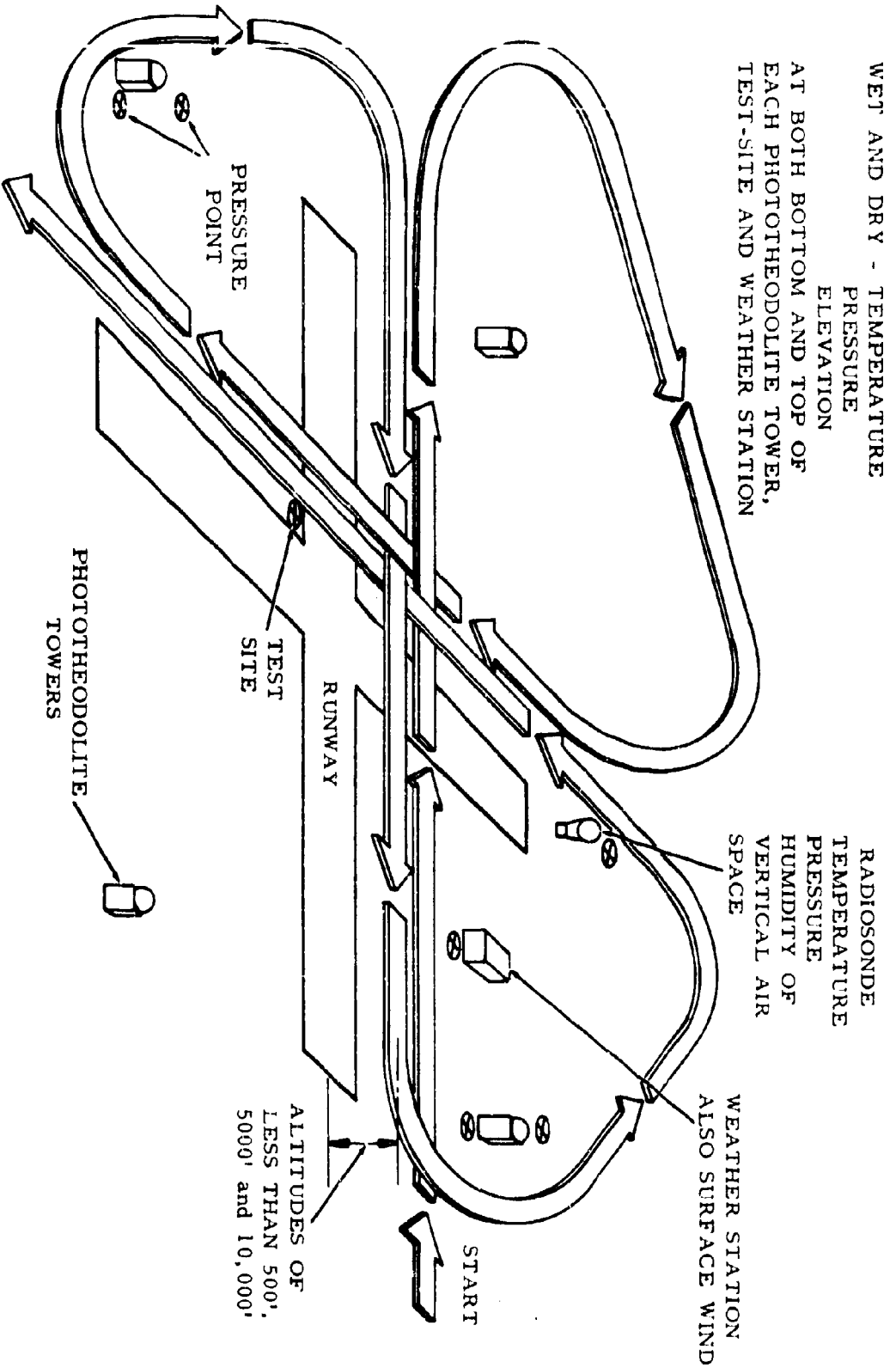


FIG. 8 AIRCRAFT FLIGHT PATH - FIELD LAYOUT

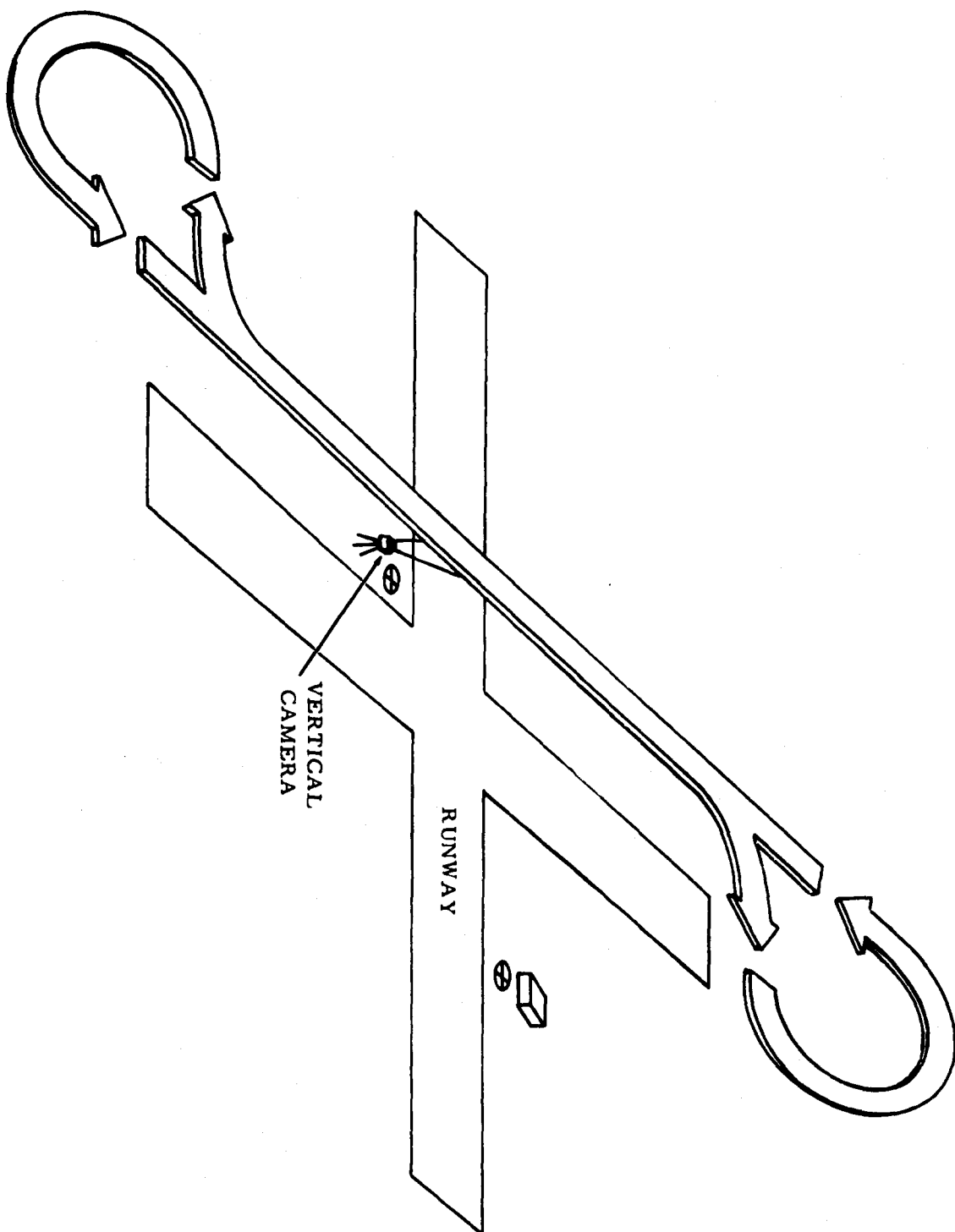


FIG. 9 AIRCRAFT FLIGHT PATH OVER VERTICAL CAMERA

### III. Tower Fly-By

The test procedure was similar to those described in Test Procedures I and II with the following exceptions:

The aircraft's flight path, Fig. 10, was over a prescribed ground track at an altitude which by visual reference appeared to the pilot to be that equal to the tower height. An observer in the tower would note and record the angular displacement of the aircraft with respect to a scribed scale or reference mark at the instant it passed the tower.

### IV. Radar Tracking/Pressure Survey

The test procedures prior to takeoff, at low-level reference speed following takeoff, just prior to landing, and after landing were the same as those described in Test Procedures I and II.

Following the initial low-level flights, the aircraft ascended directly to the scheduled test altitude. The aircraft was flown at a constant speed in straight and level flight, and a pressure survey of the test area, as shown in Fig. 11, was made based on flying a constant indicated altitude while being tracked by a precision radar system.

The aircraft was then flown at the same indicated test altitude through its entire speed range using the flight pattern shown in Fig. 11 to facilitate the computation of airspeed.

Precision radar was used to determine the absolute geometric height of the aircraft during the pressure survey and all altitude test points.

### V. Radar Phototheodolite/Radiosonde

This method is similar to that described in Test Procedure IV with the exception that the ambient pressure at altitude was derived from atmospheric information telemetrically obtained from a precision radar-tracked, specially calibrated radiosonde.

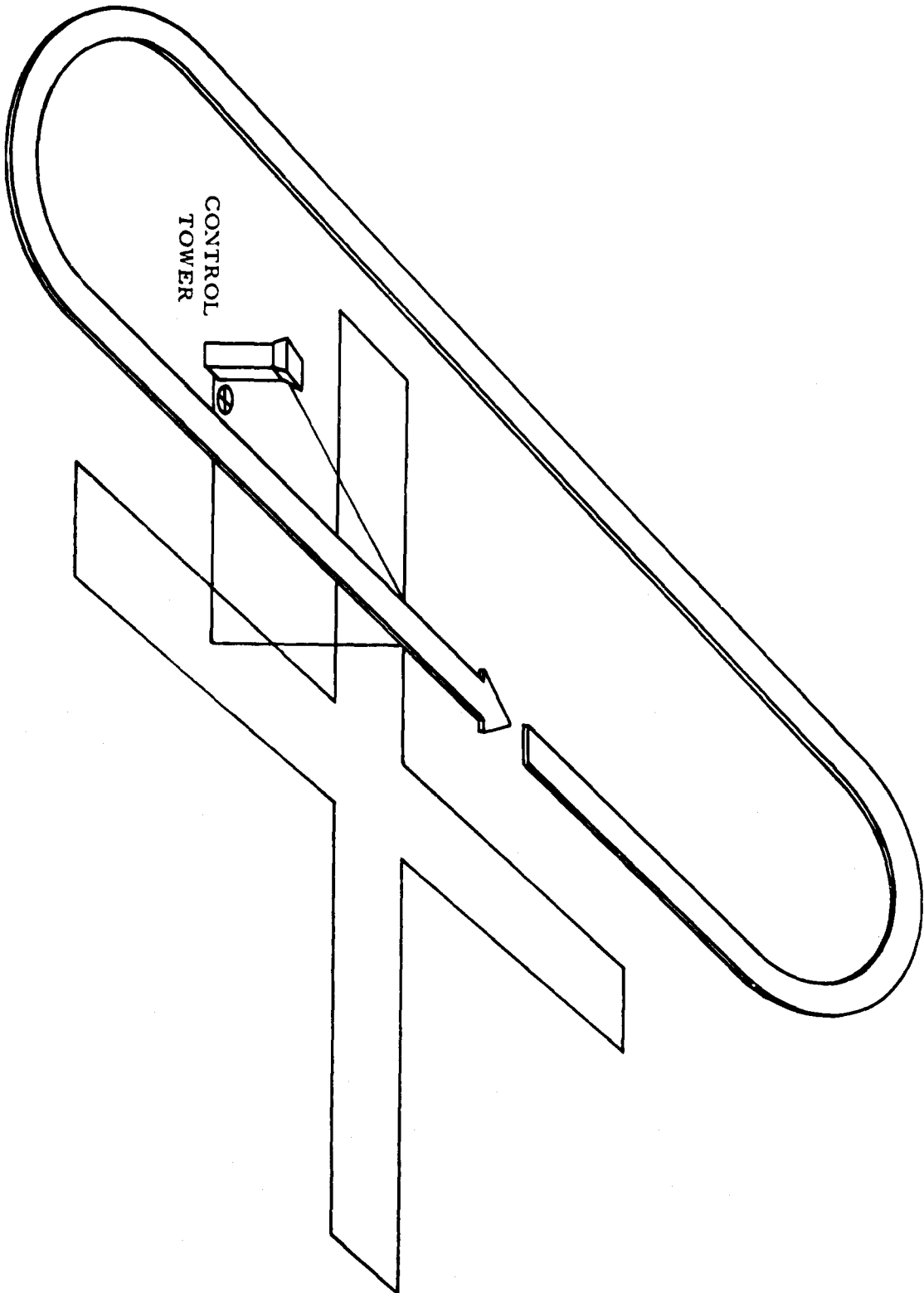


FIG. 10 AIRCRAFT FLIGHT PATH FOR TOWER FLY-BY

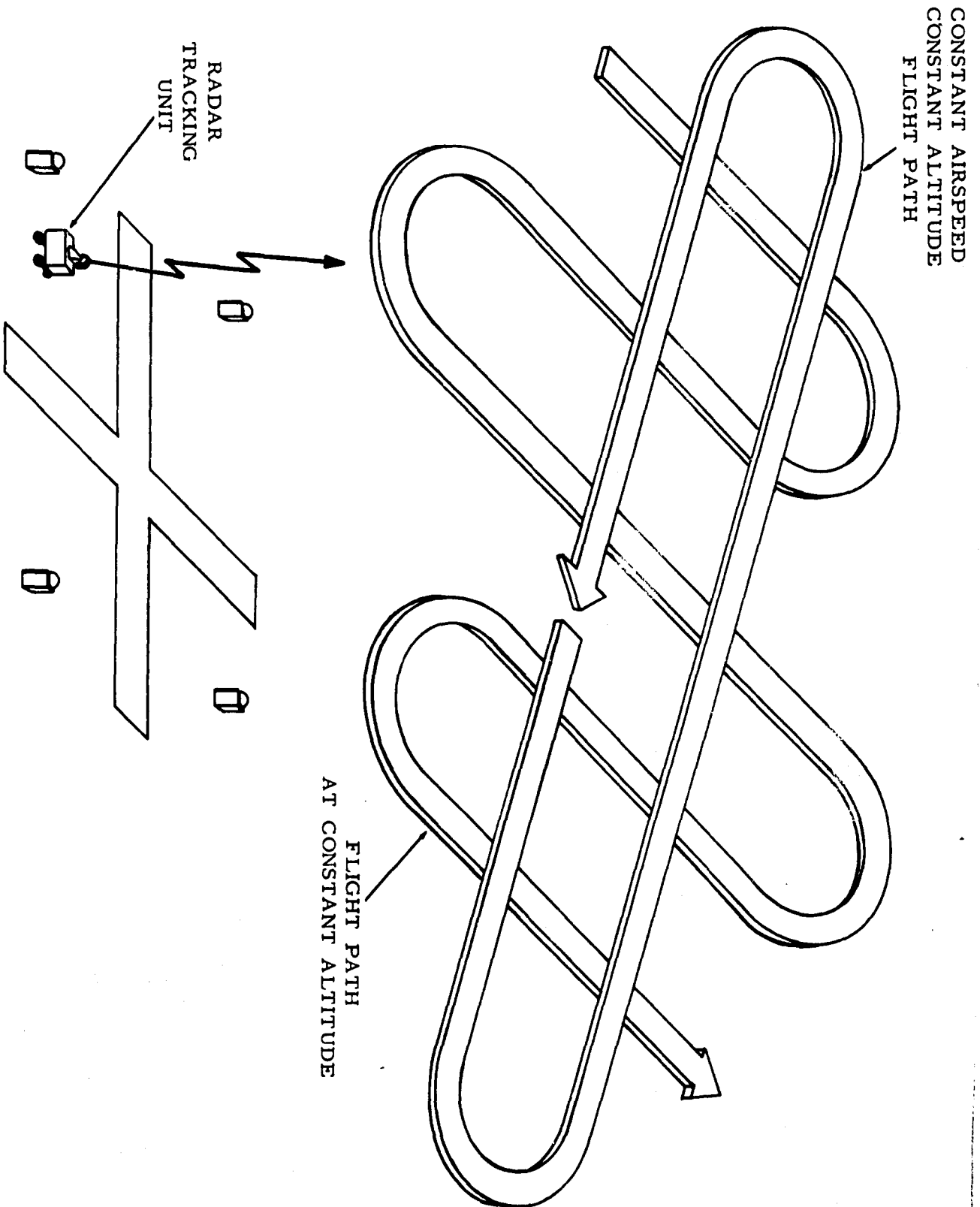


FIG. 11 PRESSURE SURVEY AT ALTITUDE

## VI. Pacer/Chase

The test aircraft, after the ground and low-altitude reference phase described in Test Procedures I, II or III, ascended to the given test altitude. It then flew by a slower moving aircraft at increasing speed increments generally following the pattern shown in Fig. 12. These overtakes were based on visual reference of the pilot in the overtaking aircraft. Attempts were made to maintain a minimum horizontal separation between the two aircraft during the overtake so that an observer in one of the aircraft involved could determine the relative vertical separation at the instant of overtake.

Recordings of all pertinent instruments in both aircraft were made at the instant of passing.

## VII. Temperature Profile Survey

The test procedure prior to takeoff, at low-level reference speed following takeoff, just prior to landing, and after landing was the same as that described in Test Procedures I and II.

Following the initial low-level flights, the aircraft ascended in incremental altitudes up to the scheduled test altitude as shown in Fig. 13. At each of these incremental altitudes the aircraft was flown at low-level reference speed velocities and conditions.

The aircraft was then flown at the same indicated test altitude throughout the entire speed range using the flight pattern shown in Fig. 13.

After the last speed point, the aircraft descended in altitude increments in the same manner as that preceding the altitude tests.

## VIII. Density Profile Survey

The test procedure was similar to that noted in Test Procedure VII.

## TEST EQUIPMENT

### TV-2 Pacer Aircraft

The test aircraft, Fig. 14, was a modified jet trainer specially equipped for this program. The special modification included: (a) nose boom, (b) trailing cone assembly with reel,

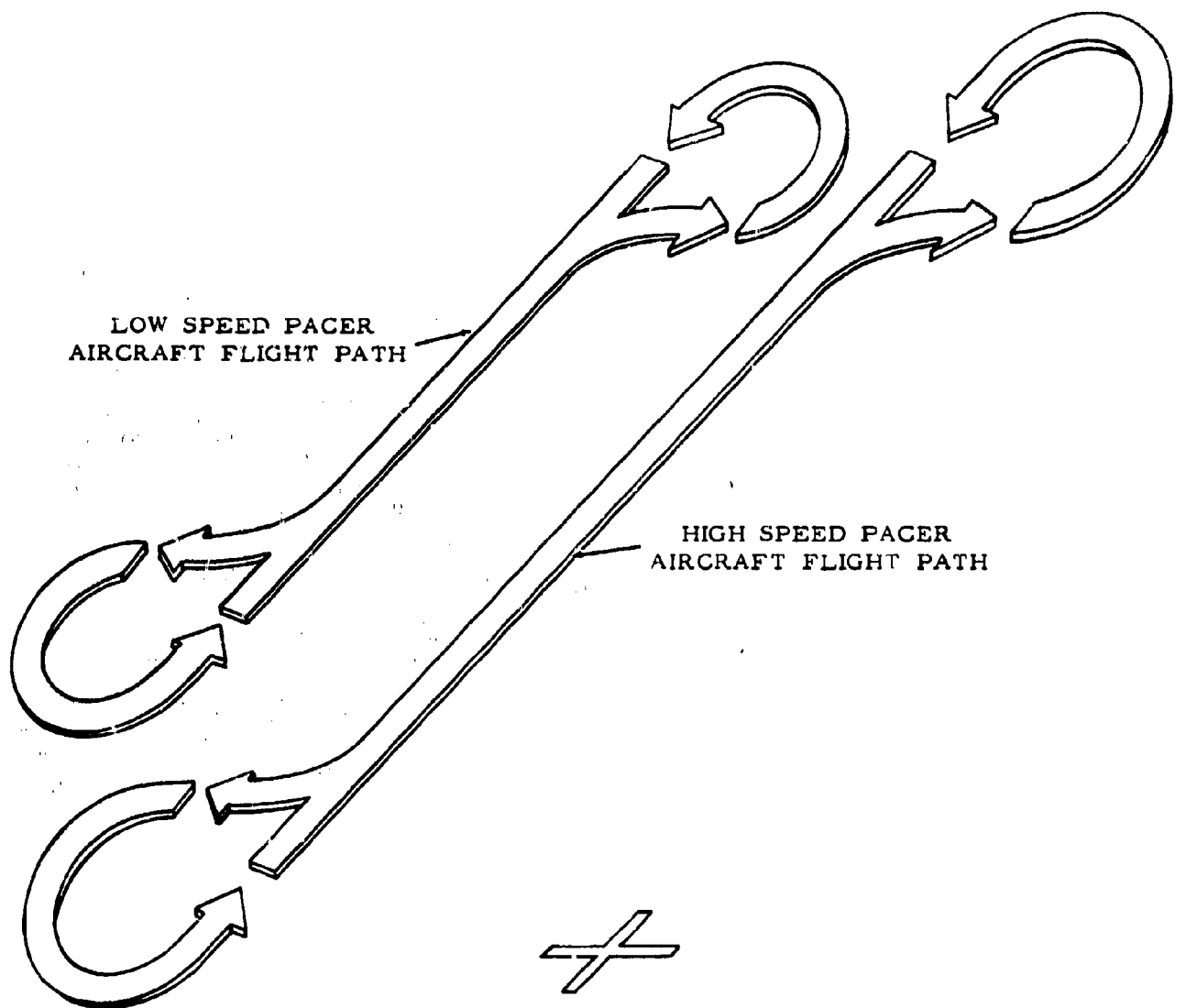


FIG. 12 AIRCRAFT OVERTAKE METHOD



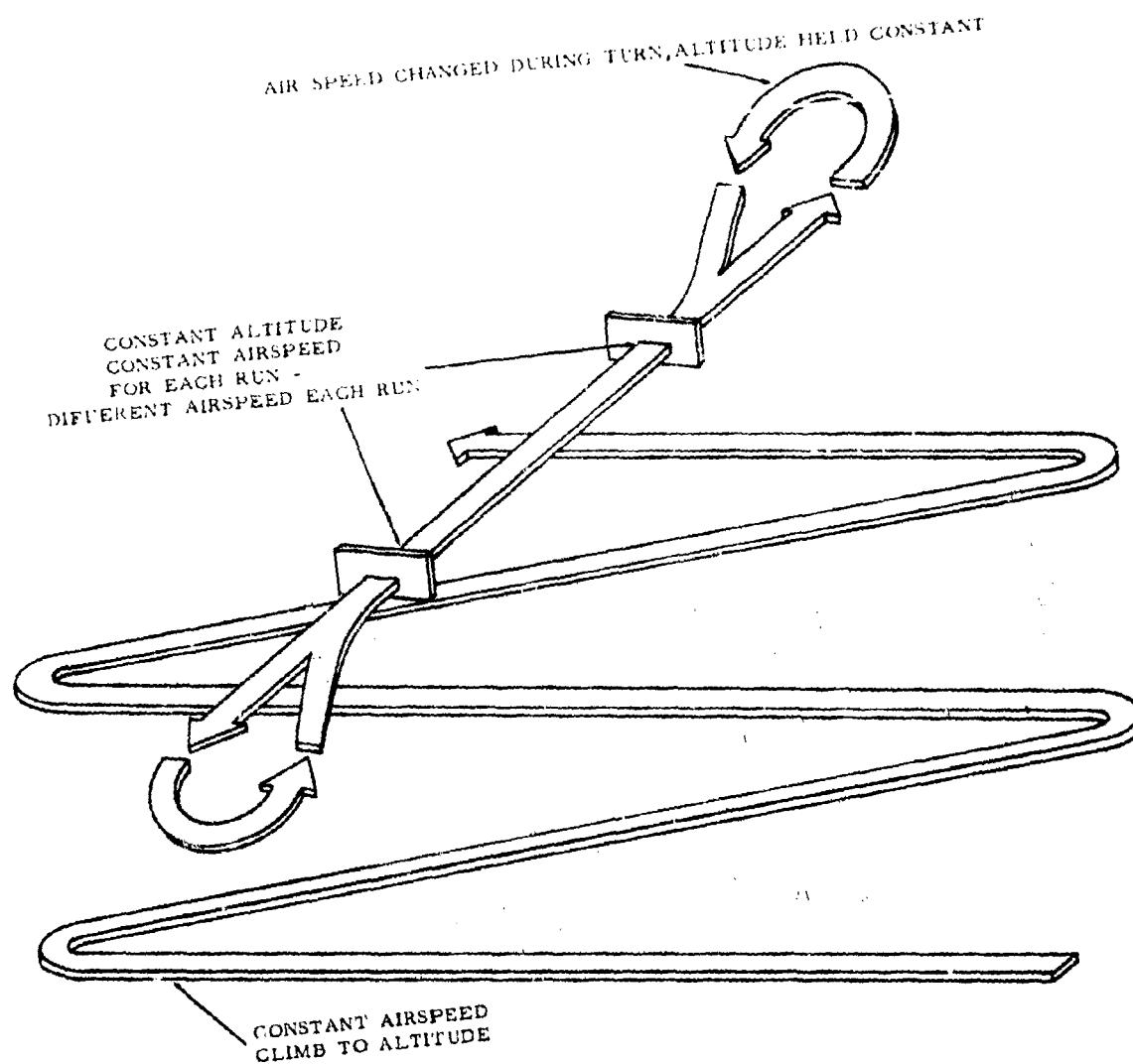


FIG. 13 FLIGHT PATTERN AT VARYING AIRSPEED  
AND CONSTANT ALTITUDE

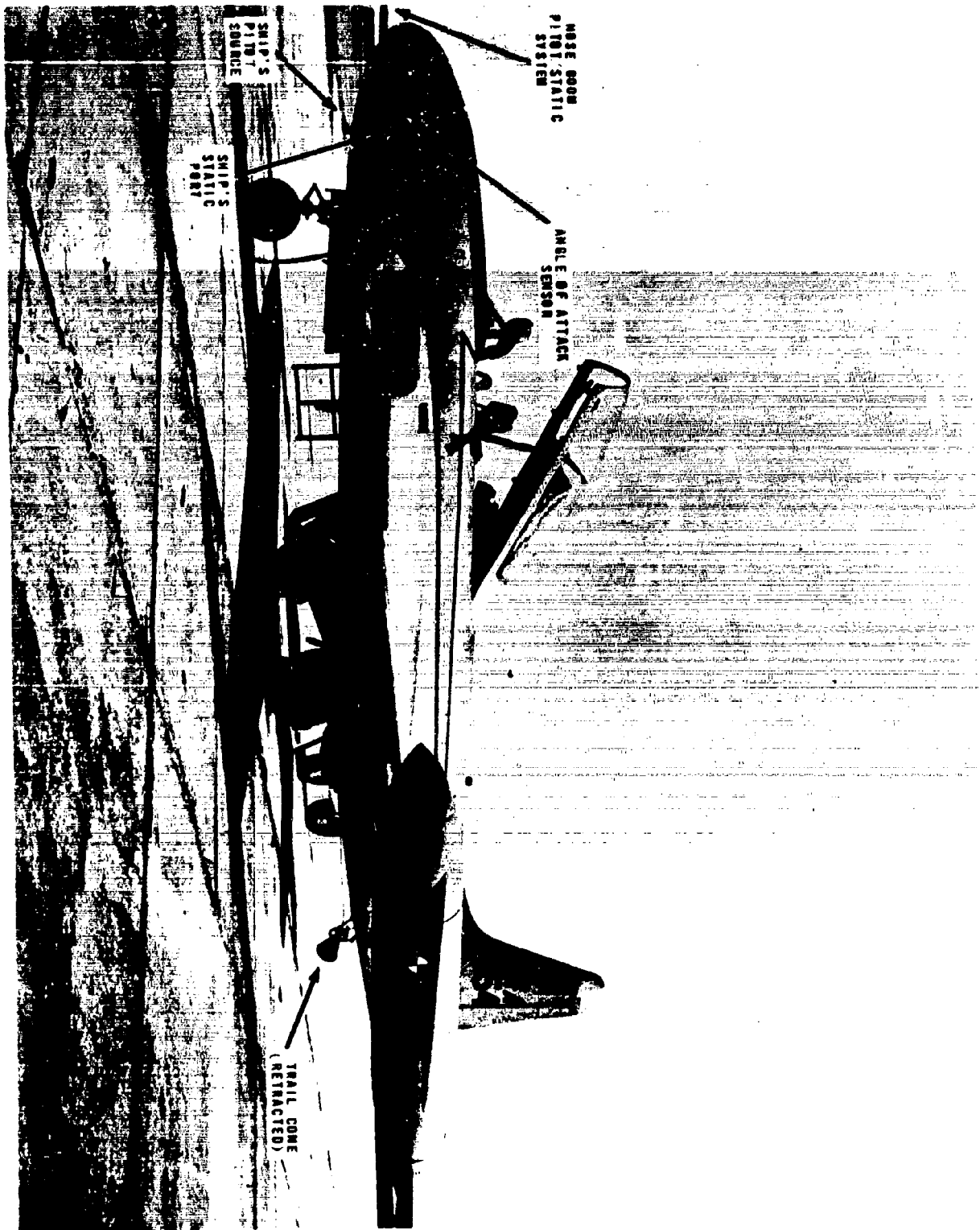


FIG. 14 TV-2 TEST AIRCRAFT

(c) special flight sensors (described below), (d) instrumented photopanel observer seat (e) special radar transponder equipment, and (f) telemetric digital clock.

The related test parameters were measured by the sensor and readout equipment noted below:

1. Ship's Indicated Altitude

The ship's normal flush static ports were connected to a selected low-hysteresis altimeter with vibrator. The repeatability of the selected altimeter was  $\pm 10$  feet based on special calibrations. This instrument and other photopanel instruments are shown in Fig. 15.

All pressure instruments were precision-calibrated by NAFEC against standards whose accuracy of  $\pm 0.0011$  inch Hg., is traceable to the National Bureau of Standards' (NBS) pressure references.

2. Ship's Indicated Airspeed

The indicated airspeed of the ship's normal pitot/flush static system was connected to a precision-calibrated, low-hysteresis airspeed indicator.

3. Nose Boom Indicated Altitude

The static pressure ports of the Kollsman pitot/static head were connected to an altimeter of the type noted in item 1, and a high resolution, servo-driven, absolute pressure transducer. The servo-driven transducer, whose matched tape scale of 165 inches in length, had an absolute accuracy of  $\pm 0.004$  inch Hg., and a repeatability and resolution of 0.002 inch Hg.

4. Nose Boom Indicated Airspeed

The dynamic pressure sensed by the special nose boom was connected to a precision-calibrated airspeed indicator similar to that used for item 2, and to a differential pressure transducer similar to the servo-driven absolute described in item 3.

5. Trailing Cone System Indicated Altitude

The sensed static pressure of the trailing cone system was instrumented in the manner prescribed for item 3.

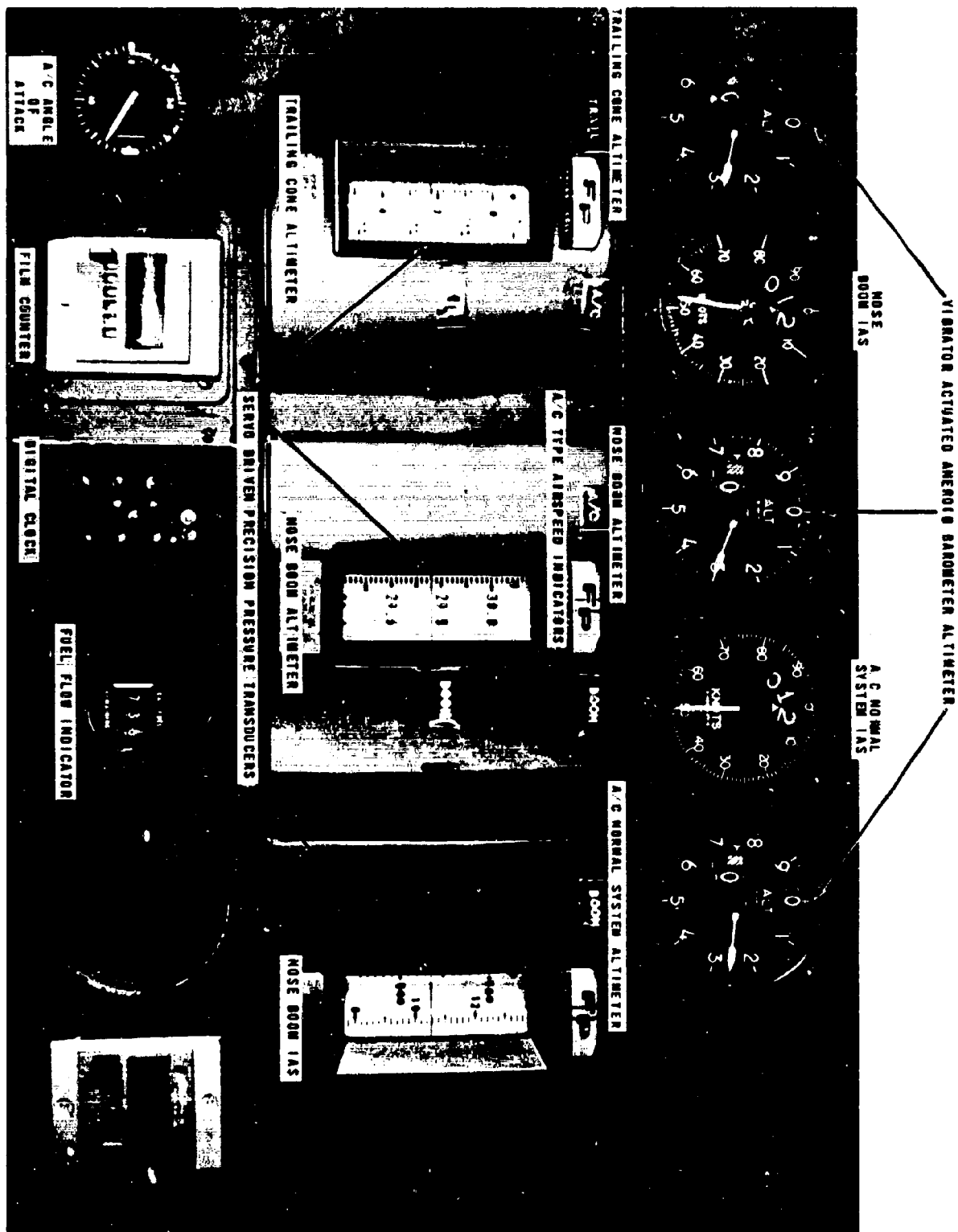


FIG. 15 PHOTOPANEL OF TV-2

## 6. Air Temperature

The stagnation air temperature was sensed by an aerodynamically-compensated temperature probe with a recovery factor equal approximately to unity and readout in degrees centigrade on a dial indicator. The ability of the systems to accurately indicate temperature was  $\pm 0.1^{\circ}\text{C}$  with a guaranteed recovery factor of 0.995 of calibration throughout the entire flight envelope.

## 7. Fuel Flow

The total fuel flow was sensed by the normal aircraft fuel meter and presented digitally on the photopanel.

## 8. Angle of Attack

A null-seeking pressure transduction-type angle-of-attack sensor and associated dial presentation was calibrated to  $0.2^{\circ}$  angular displacement.

## F8C Pacer Aircraft

The Navy-furnished F8C, Fig. 16, was a specially instrumented supersonic fighter-type aircraft. Included in the special instrumentation were: (a) instrumented nose boom, (b) tail-mounted trailing cone system with internally stored power-driven reel, (c) special radar transponding equipment, and (d) internally mounted photopanel. The parameters read out on the photopanel, Fig. 17, were similar to that of the TV-2 pacer aircraft.

### 1. Ship's Indicated Altitude

The photopanel presentation was a sensitive precision-calibrated, aneroid barometric altimeter, the calibration of which was traceable to NBS pressure reference standards. This unit was in parallel to the ship's normal altimeter located in the pilot's panel.

### 2. Ship's Indicated Airspeed

A calibrated aircraft airspeed indicator was hooked in parallel to the aircraft's normal dynamic pressure system.

### 3. Nose Boom Indicated Altitude

The readout of the nose boom sensed static pressure was similar to that employed for the ship's system.



FIG. 16 F8C TEST AIRCRAFT

#### 4. Nose Boom Indicated Airspeed

The sensed dynamic pressure of the nose boom was read out on a standard precision-calibrated airspeed indicator.

#### 5. Trailing Cone System Indicated Altitude

The sensed static pressure was read out on a selected precision-calibrated aneroid barometric altimeter similar to the ship's static system. In addition, a second altimeter was located above the pilot's normal flight panel for pilot usage.

#### 6. Nose Boom/Trailing Cone Indicated Airspeed

The sensed total pressure of the nose boom and sensed static pressure of the trailing cone system were coupled to a precision airspeed indicator.

#### 7. Angle of Attack

A calibrated vane-type angle of attack sensor was employed to determine aircraft angle of attack. Other existing instrumentation, shown in Fig. 17, was not employed for this project.

### Ground Based Equipment

The following equipment was employed where applicable to determine geometric altitude of the test aircraft or to obtain atmospheric information:

#### 1. NAFEC Phototheodolite System

The phototheodolite system, Fig. 18, was employed to determine the geometric height and aircraft ground speed for all tests up to 10,000 feet which occurred at NAFEC. The reported accuracy of this system as employed in this program was  $\pm 2.0$  feet in elevation and  $\pm 3.0$  feet per second (fps) in computed ground speed.

#### 2. Vertical Aerial Camera

The aerial camera, Fig. 19, was used to obtain low-level aircraft altitudes where the phototheodolite system was inoperative or not available. A detailed description of this method is contained in Reference AC. The accuracy of this method, as verified by the NAFEC phototheodolite system, was within 0.5 feet of the theodolite data.

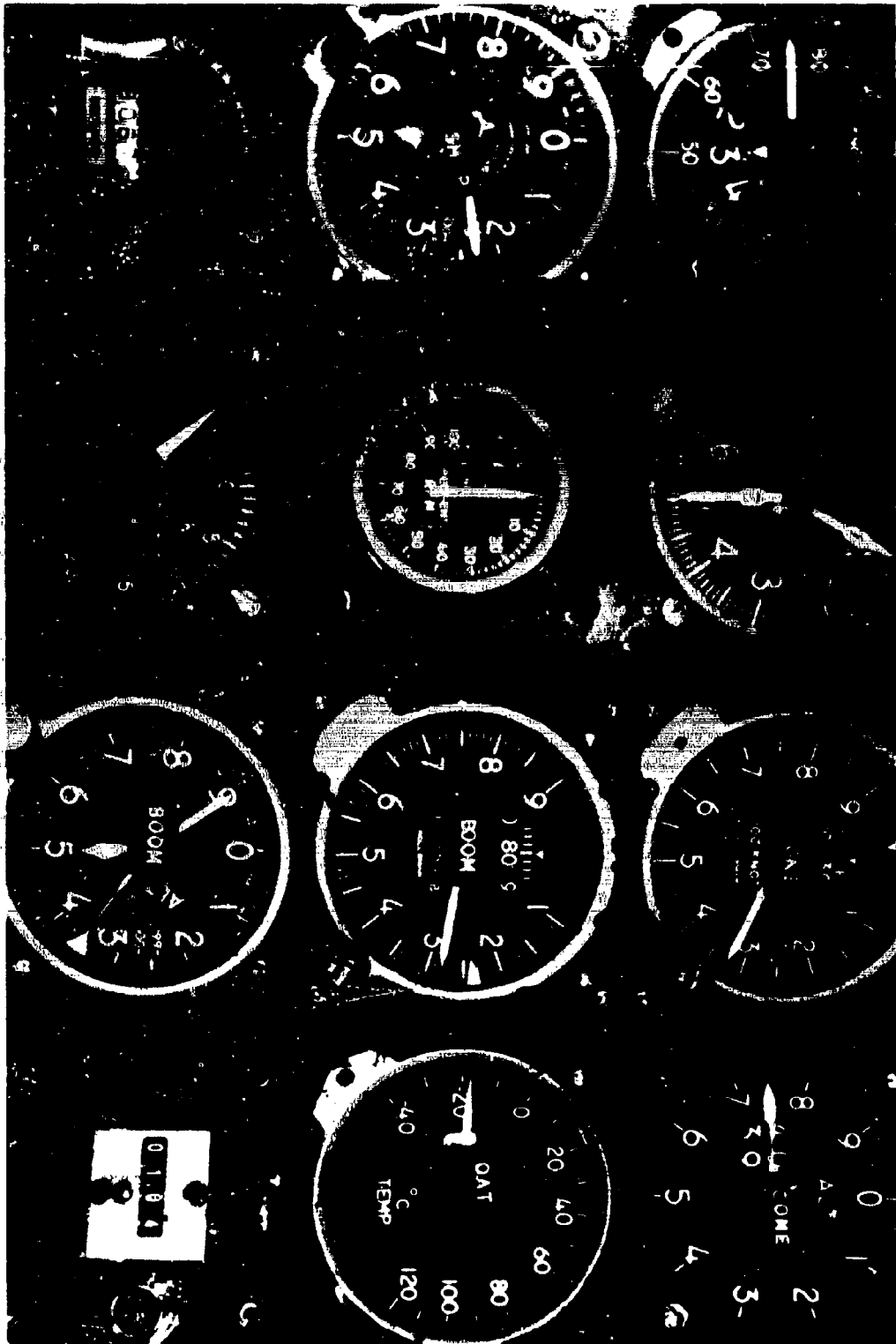
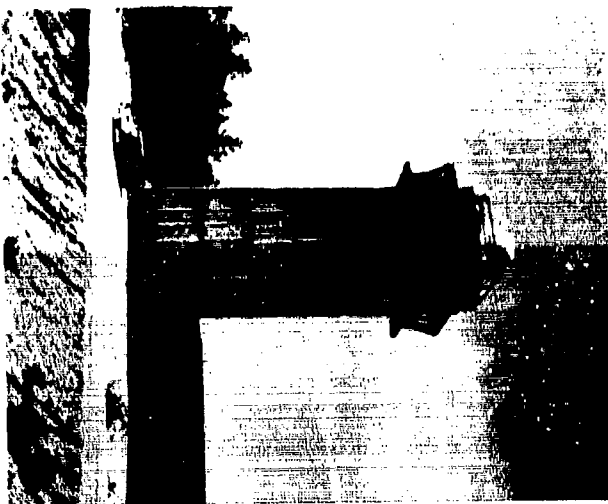
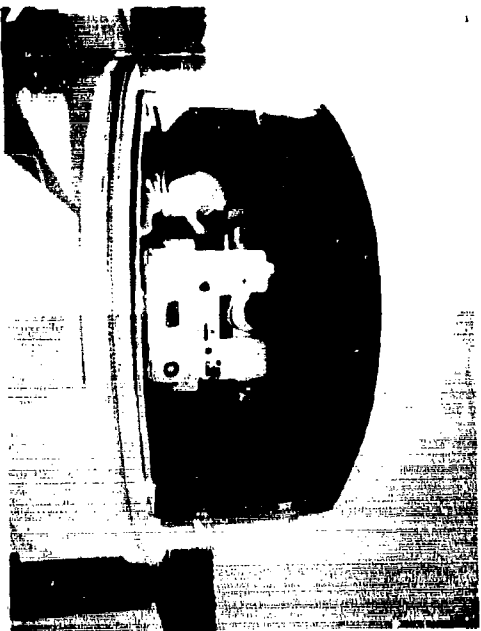


FIG. 17 PHOTOPANEL OF P8C

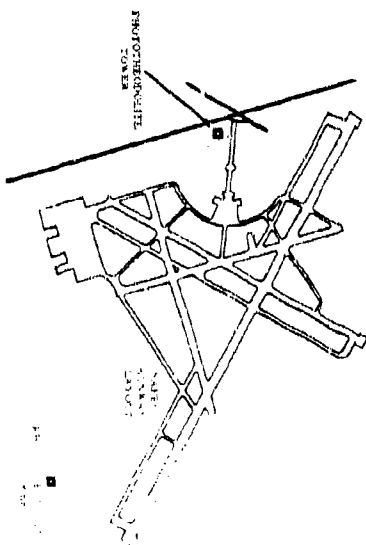




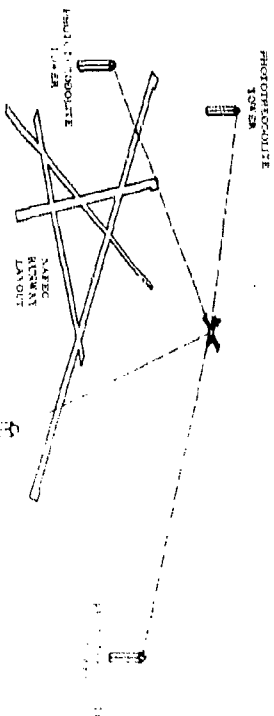
THE TOWER



THE TOWER



PHOTORECOGNITION  
TOWER



PHOTORECOGNITION  
TOWER

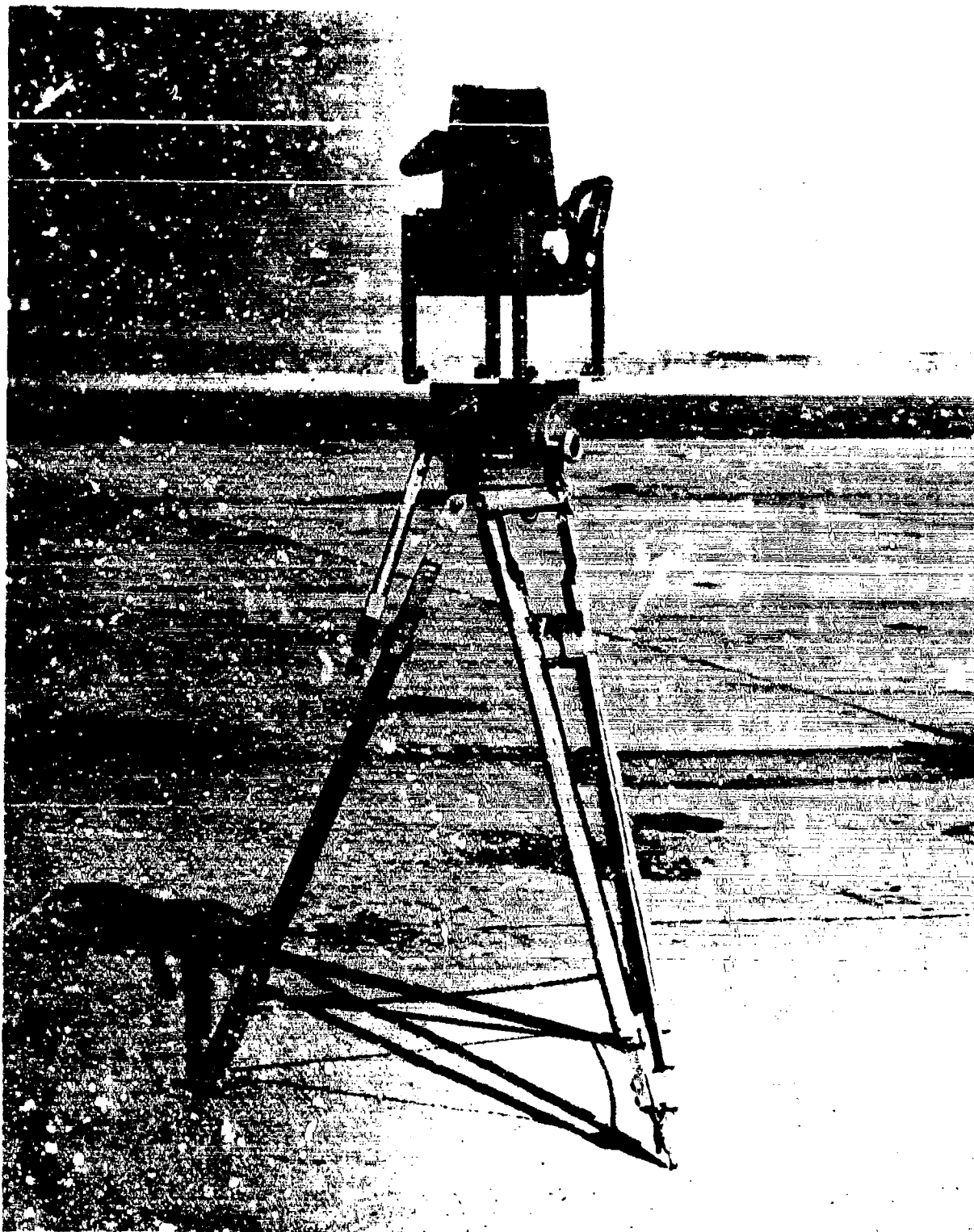


FIG. 19 AERIAL CAMERA

### 3. NAFEC Tracking Radar System

The X-band radar system, Fig. 20, was employed to obtain geometric elevation and ground speed of the test aircraft during the high-altitude tests at NAFEC. The reported accuracy of this system is 25 feet in determining height.

### 4. NATC Radar/Phototheodolite System

The NATC system employs a radar-coupled acquisition phototheodolite system for determining the geometric height of the aircraft. The accuracy of this system is not known, but would be dependent on the optical limitation due to the equipment and a given atmospheric condition. Data reduction using this system was accomplished by NATC and is contained in Reference R.

### 5. Radiosonde

The atmosphere was surveyed by a calibrated radiosonde similar to that shown in Fig. 21. The accuracy of the aneroid system was 0.01 inch Hg., and that of the temperature sensing systems 0.5°C.

### 6. Barometer

The barometer shown in Fig. 22 was the type used at each of the ground-measuring stations noted in Fig. 8. These devices were calibrated against a known standard prior to and after their application to this project.

### 7. Air Temperature/Humidity

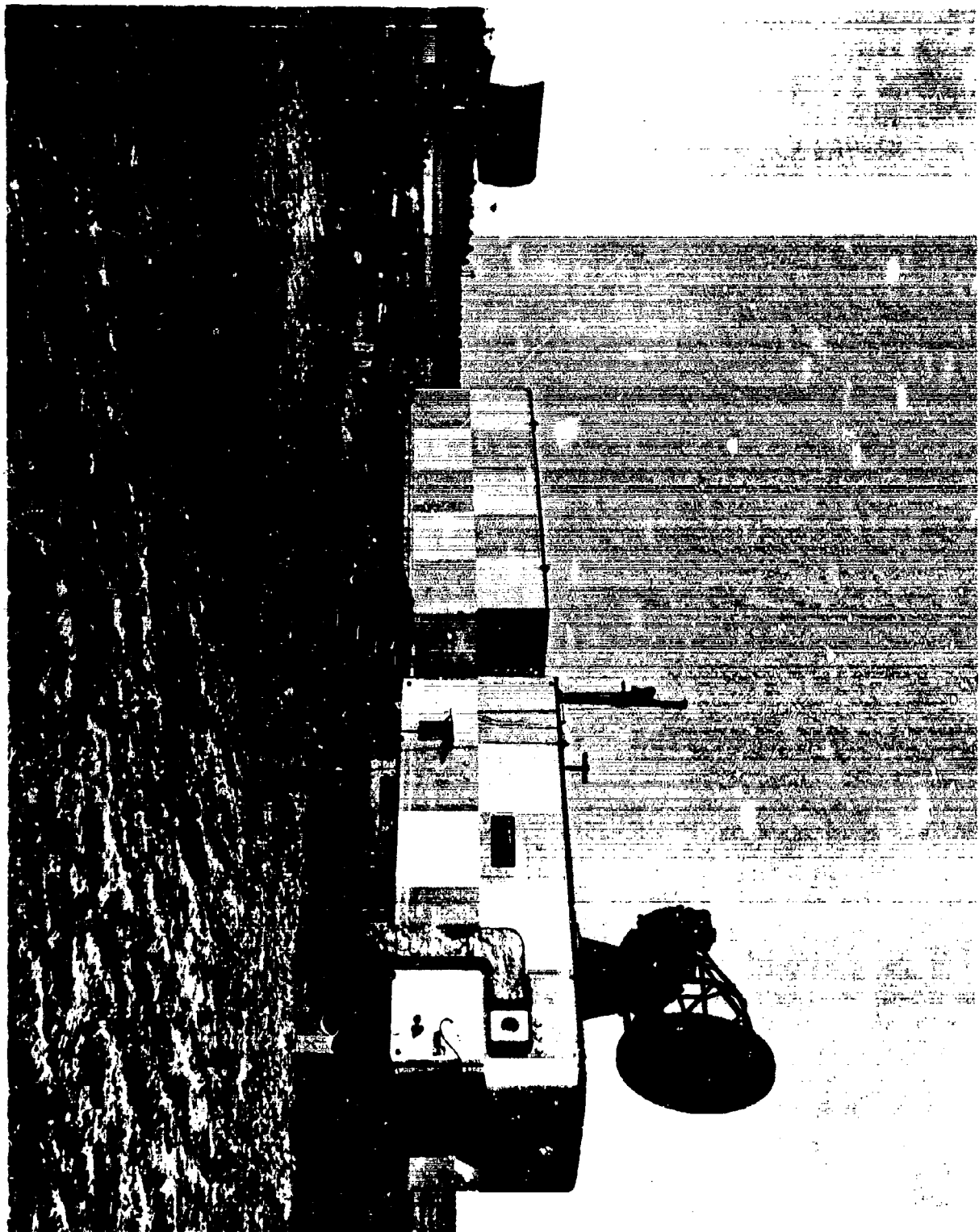
The wet and dry-bulb temperatures at each of the ground-measuring stations were obtained by use of the self-operating psychron unit shown in Fig. 23. This unit was calibrated and has an accuracy of  $\pm 0.1^{\circ}\text{F}$ .

## METHOD OF ANALYSIS

Position error, as defined herein, is the difference between the local pressure at the static ports and the free stream ambient pressure. Therefore, to derive this difference,  $\Delta P$ , one must compute the value of the local pressure and that of the free stream ambient.

The value of the local pressure was obtained by three independent methods with respect to the readout instruments:

FIG. 20 X-BAND RADAR (TARE)



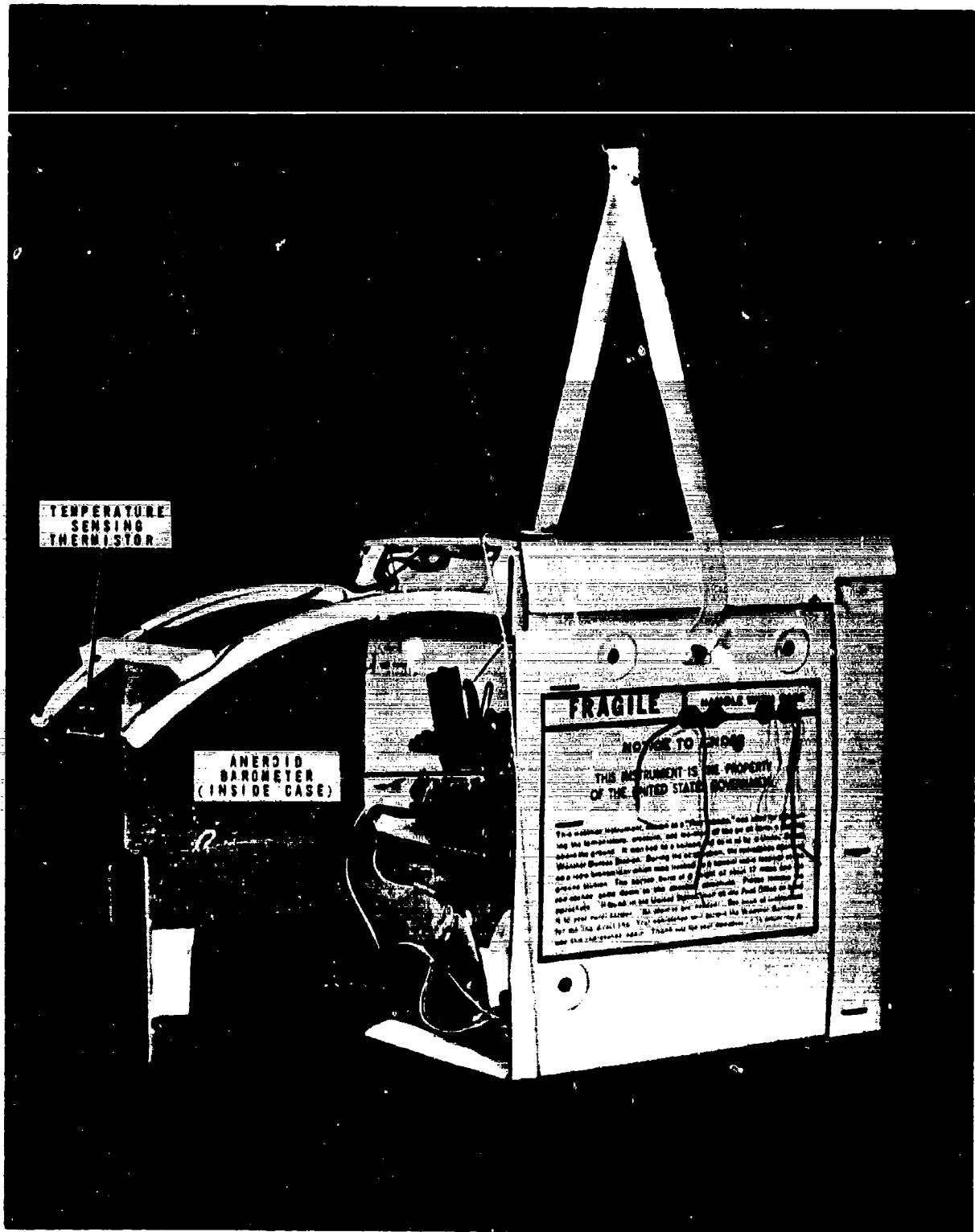


FIG. 21 RADIOSONDE

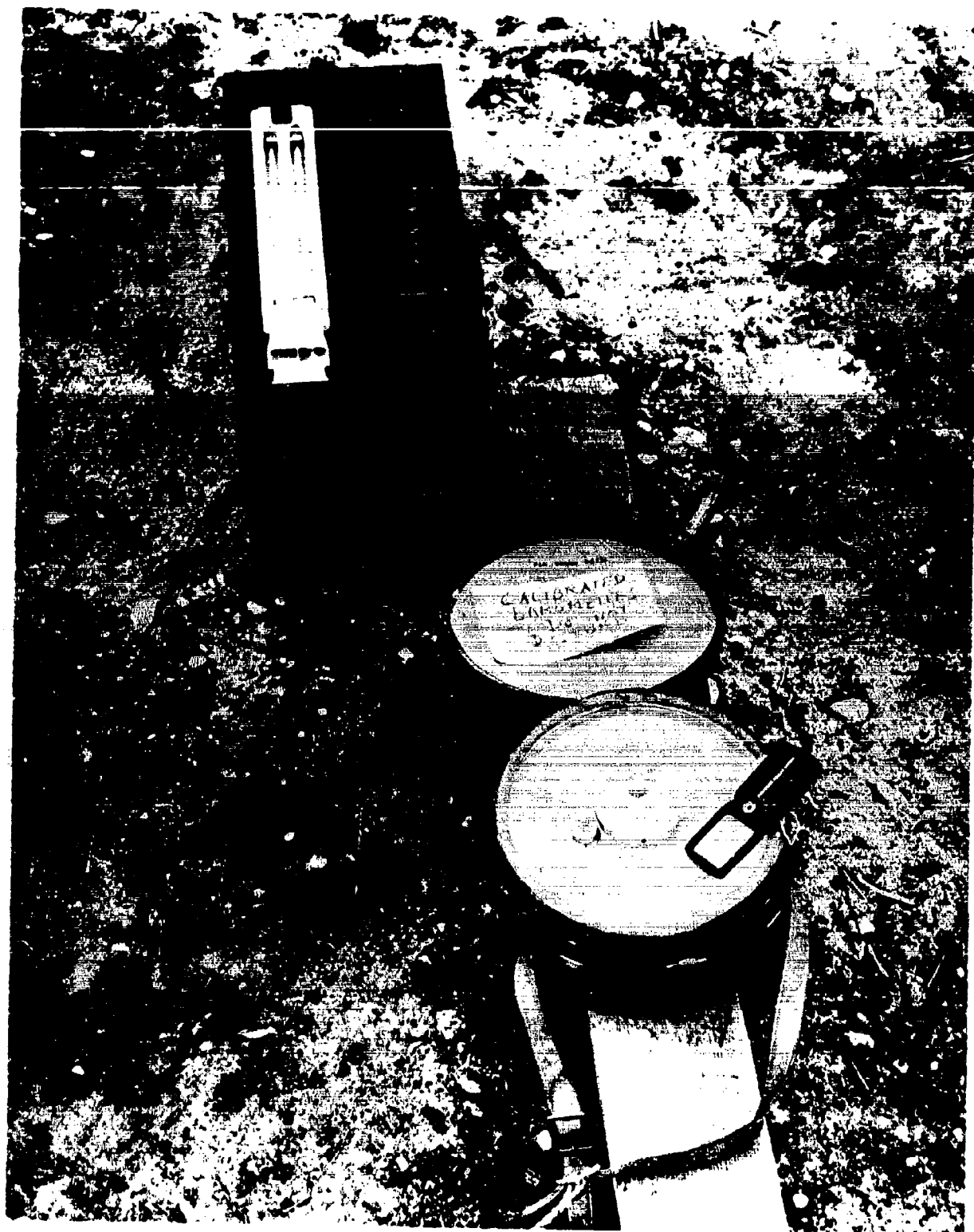


FIG. 22 BAROMETER

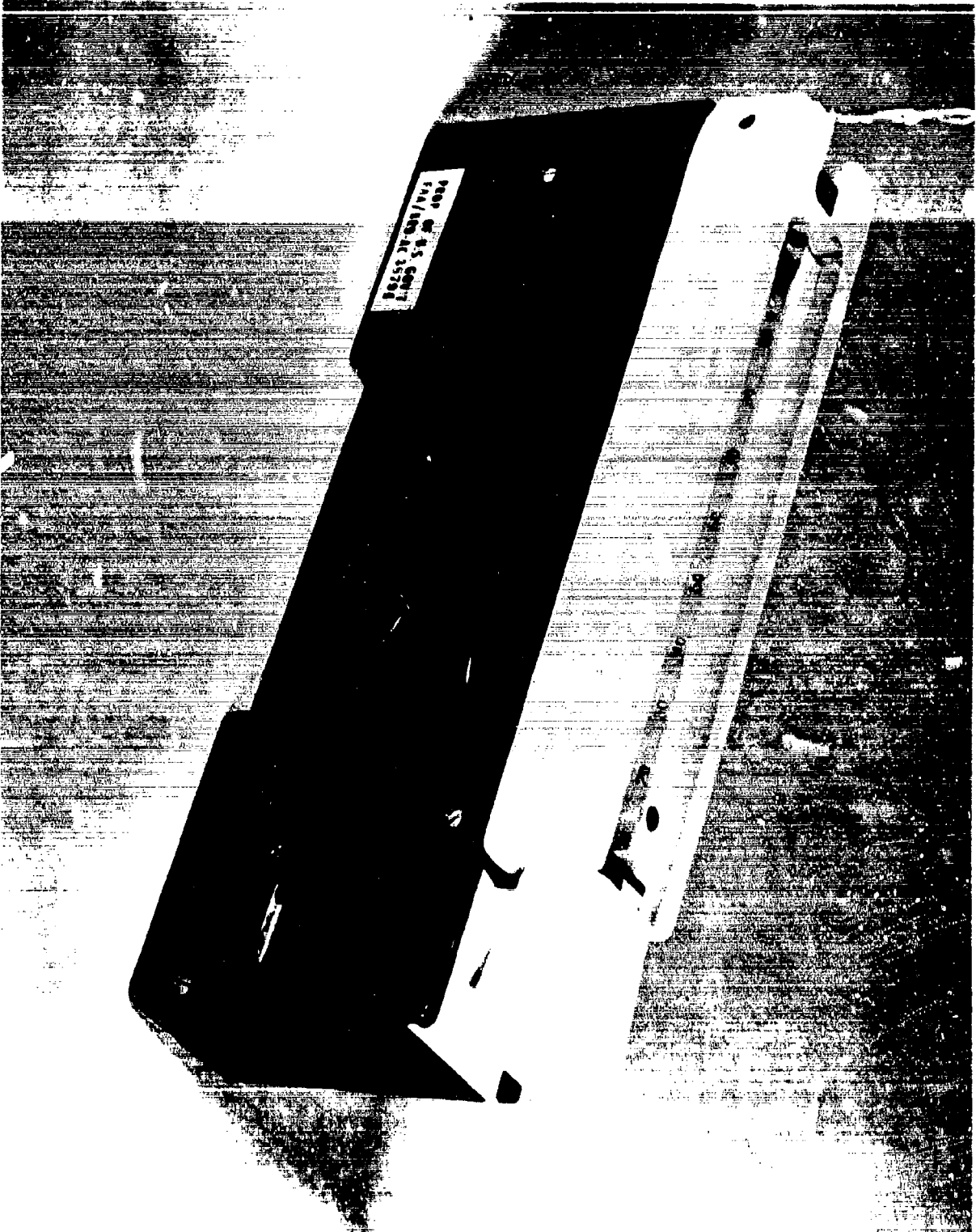


FIG. 23 PSYCHRON UNIT

The first method was to correct the absolute value obtained for the indicated local static pressure,  $P_{IT}$  (trailing cone system altitude), for known scale error. The scale error corrections included both the precision calibration term and any bias which was reflected during the preflight calibration. This resultant value is defined as the absolute calibrated local pressure at the static pressure ports,  $P_{IC}$ .

$$P_{IC} = P_{IT} - (P_{GP} + P_B) \quad (1)$$

where  $P_{IC}$  = Calibrated local pressure,  
 $P_{IT}$  = Indicated local pressure,  
 $P_{GP}$  = Calibration correction term of scale for a given value of  $P_{IT}$ ,  
 $P_B$  = Preflight calibration bias.

The second method was to correct the indicated ground check reading for any difference between indicated ground station pressure and known ground station pressure, and then subtract from this pressure value the indicated pressure at the test condition. The resultant value is defined as change in calibrated local pressure of the trailing cone system's static ports,  $\Delta P_{IC}$ .

$$\Delta P_{IC} = [P_{GI} - (P_{GI} - P_G)] - P_{IT} \quad (2)$$

where  $\Delta P_{IC}$  = Change in calibrated local pressure,  
 $P_{GI}$  = Indicated ground station pressure,  
 $P_G$  = Known ground station pressure.

The third method was a modification of the second procedure where the indicated local pressure,  $P_{IR}$ , at a given reference speed at the test altitude was used in place of the indicated ground pressure reading.

$$\Delta P_{IC} = P_{IR} - P_{IT} \quad (3)$$

where  $P_{IR}$  = Indicated local pressure at a given reference speed.

The value of the free stream ambient pressure at the test condition altitude was determined by five different methods dependent upon attainable accuracy of observed information.



The first method consisted of computing the corrected station pressure reading for each of the observed ground readings. The observed reading was corrected for scale pressure and temperature error, then extrapolated to the station pressure ground elevation,  $P_{GC}$ , using the model atmospheric lapse rate. The extrapolated values of  $P_{GC}$  were then averaged. The ambient pressure at test altitude,  $P_C$ , was derived by subtracting from the averaged value for station pressure,  $\bar{P}_{GC}$ , the computed change in pressure,  $\Delta P_C$ , as a function of density.

$$P_C = \bar{P}_{GC} - \Delta P_C \quad (4)$$

$$\bar{P}_{GC} = \frac{\sum_1^N [P_{GI} - (P_{GP} + P_{GT} + P_K \Delta h)]}{N} \quad (5)$$

$$\Delta P_C = - \rho g \Delta H \quad (6)$$

$$\rho_C = \rho_S \frac{\bar{P}_{GC}}{P_S} \times \frac{T_S}{T_{GC}} \quad (7)$$

where

- $P_C$  = Computed pressure at test altitude,
- $\bar{P}_{GC}$  = Mean computed ground station pressure,
- $\Delta P_C$  = Change in computed station pressure due to  $\Delta H$ ,
- $P_{GT}$  = Calibration correction factor due to ambient temperature of the barometer,
- $P_K$  = Rate of change in pressure at station elevation based on a model atmosphere,
- $\Delta h$  = Difference in elevation between observed ground reading and station elevation,
- $N$  = Number of readings
- $\rho_C$  = Computed local density of air mass,
- $g$  = Local gravity,

$\Delta H$  = Difference in geometric height of station elevation and test altitude,

$\rho_3$  = Model atmosphere density for a given elevation,

$P_g$  = Standard day pressure at station elevation,

$T_g$  = Standard day air temperature at station elevation,

$T_{GC}$  = Mean ground station temperature.

The second method of computing ambient pressure at the test altitude was to determine the mean pressure lapse rate,  $\bar{P}_{KC}$ , based on observed corrected barometric pressure,  $P_{BC}$ , measured at various elevations. This computed lapse rate was multiplied by the change in elevation,  $\Delta H$ , from the closest accurately determined barometric pressure and the resultant value subtracted from the barometric pressure.

$$\Delta P_C = P_{BCN} - \bar{P}_{KC} \Delta H \quad (8)$$

$$\bar{P}_{KC} = \frac{\sum_{i=1}^N P_{BC} - P_{BC'}}{N} \quad (9)$$

where  $P_{BCN}$  = Observed corrected barometric pressure closest to the test altitude,

$\bar{P}_{KC}$  = Mean computed pressure lapse rate,

$P_{BC}$  = Observed corrected barometric pressure of the base of a given air column,

$P_{BC'}$  = Observed corrected barometric pressure at some known point in a given air column.

A third method of obtaining a value for ambient pressure at altitude was to assume a mean reference pressure,  $\bar{P}_R$ , based on the horizontal profiling of the atmosphere covered in Test Procedure IV. The value was then corrected by the model atmospheric lapse rate for any difference between the test altitude and the altitude at which the mean reference pressure was obtained. The lapse rate used was that applicable for the reference pressure altitude.

$$P_C = \bar{P}_R - P_K \Delta H \quad (10)$$

$$\bar{P}_R = \frac{\sum_1^N P_R}{N} + \frac{\sum_1^{N'} P_{R'}}{N'} \quad (11)$$

where  $\bar{P}_R$  = Mean ambient reference pressure,

$P_R$  = Corrected reference pressure based on horizontal pressure survey preceding test,

$P_{R'}$  = Corrected reference pressure based on horizontal pressure survey following test,

$N$  = Number of readings preceding test,

$N'$  = Number of readings following test.

An additional method of obtaining ambient pressure at altitude was by computing the pressure by Boyle's Law for an ideal gas. The temperature employed was that computed based on the vertical profile of the air column temperature.

$$P_C = \rho_S^{RT_C} \quad (12)$$

where  $R$  = Gas constant for dry air,

$T_C$  = Computed temperature at test altitude based on vertical profile of air column temperature.

The final method employed to service the ambient pressure at the test altitude was to compute the density lapse rate as a function of geometric altitude, then use the computed temperature to calculate the ambient pressure.

$$P_C = \rho_C^{RT_C} \quad (\text{Assuming air as a perfect gas}) \quad (13)$$

$$\rho_C = \rho_{GC} - \sum_G^T \rho_S \frac{P}{P_S} \times \frac{T_S}{T} \quad (14)$$

where  $\rho_{GC}$  = Computed density at the base of the air column.

There were two methods employed to obtain calibrated airspeed of the test aircraft depending upon available test observations and procedures.

The first method was to compute the calibrated airspeed based on the average of tracked ground speed based on flight paths which were  $180^\circ$  with respect to each other at the same indicated velocity. The equivalent dynamic pressure was computed by Bernoulli's relation of pressure to velocity and density.

$$V = \frac{V_{G1} + V_{G2}}{2} \quad (15)$$

where  $V$  = Calibrated velocity of aircraft,

$V_{G1}$  = Tracked ground speed in direction A,

$V_{G2}$  = Tracked ground speed in direction A +  $180^\circ$ ,

and  $q_C = \frac{1}{2} \rho V^2$  (for incompressible flow) (16)

where  $q_C$  = Dynamic calibrated pressure.

The second method of deriving calibrated airspeed was by correcting the indicated airspeed for instrument and position error. The position error of the ship's system or nose boom system was assumed to be the difference between sensed static of the particular system and the trailing cone static pressure.

$$V_C = V_I - [V_{IE} + (V_{CS} - V_{CC})] \quad (17)$$

where  $V_C$  = Calibrated airspeed,

$V_I$  = Indicated airspeed,

$V_{IE}$  = Scale Error of indicator,

$V_{CS}$  = Calibrated airspeed from aircraft system indication,

$V_{CC}$  = Calibrated airspeed from trailing cone indication.

G. The equivalent value of  $q_C$  for this was obtained from Reference

The Mach Number was also obtained from Reference G based on computed equivalent values of altitude and airspeed.

The position error of the trailing cone system was obtained by determining the difference between the reference value used for  $P_C$  or  $\Delta P_C$  and the related value for  $P_{IC}$  or  $\Delta P_{IC}$ .

#### TEST RESULTS AND ANALYSIS

The results shown in Fig. 24 are a composite of all validated data obtained using the TV-2 pacer aircraft at altitudes of approximately 200, 5,000, and 10,000 feet.

The position error,  $\Delta P$ , for test conditions at 200 feet was computed by solving for  $P_{IC}$  by equation (1), and  $P_C$  by equation (4), and Test Procedure I.

$$\begin{aligned}\Delta P &= P_{IC} - P_C \\ \Delta P &= [P_{IT} - (P_{GP} + P_B)] - [P_{GC} - \Delta P_C]\end{aligned}\quad (18)$$

All data shown in Fig. 24 were verified by independently solving for  $\Delta P$  using equations (2) and (6), or through equations (2) and (8).

$$\begin{aligned}\Delta P &= \Delta P_{IC} - \Delta P_C \\ \Delta P &= [P_{GI} - (P_{GI} - P_G) - P_{IT}] + \rho g \Delta H\end{aligned}\quad (19)$$

$$\Delta P = [P_{GI} - (P_{GI} - P_G) - P_{IT}] - P_{BCN} - \bar{P}_{KC} \Delta H \quad (20)$$

The position error at 5,000 and 10,000 feet was determined and verified by combining Test Procedures I and VIII.

The average change in  $\Delta P$  as a function of airspeed, initially derived by equation (3), was determined for the low-altitude tests which preceded and followed the altitude tests.

$$\sum_{1}^N \frac{P_{IR} - P_{IT}}{N} : \sum_{1}^N \frac{P_{IR} - P_{IT}}{N'} \quad (21)$$

$$\overline{\Delta P_{IC}} = \frac{\quad}{2}$$

where  $\overline{\Delta P_{IC}}$  = Mean change in calibrated local pressure between reference test speeds,

N = Number of data points at a given reference speed preceding altitude tests,

N' = Number of data points at a given reference speed after the altitude tests.

The number of useful data points for a given test condition was nominally 10. Any given graphic validated presentation for a particular velocity is the mean of these points.

The same procedure for obtaining  $\overline{\Delta P_{IC}}$  at the test altitude was employed since the first two test points at any altitude were the reference speeds. The equation, however, takes the form shown below in equation (22).

$$\overline{\Delta P_{IC}} = \frac{\sum_{1}^N P_{IR} - P_{IT}}{N} \quad (22)$$

The indicated value of local pressure R at a given test condition,  $P_{IT}$ , was corrected for any difference in altitude between the test elevation and the altitude reference speed test elevation,  $\Delta H$ . The pressure constant,  $P_{KC}$ , was that derived based on the radiosondic survey.

$$\Delta P = \overline{\Delta P_{IC}} - P_{KC} \Delta H \quad (23)$$

This resultant  $\Delta P$  was referenced to the low-level results by the difference between  $\overline{\Delta P_{IC}}$ , as derived in equations (21) and (22).

The value obtained above was validated by subtraction from the calibrated local pressure,  $P_{IC}$ , the computed absolute value of  $P_C$  as reflected in equation (13). The values of pressure and temperature to compute density were based on the atmospheric survey as defined in Test Procedure VIII.

$$\Delta P = P_{IC} - P_C$$

$$\Delta P = [P_{IT} - (P_{GP} + P_B)] - \left[ (P_{GC} - \sum_C^T e_S \frac{P}{P_S} \times \frac{T_S}{T_C}) \right] RT_C \quad (24)$$

Thus, Fig. 24, represents all data which could be validated by solving for free stream pressure at a given test condition by both a computed pressure lapse rate and a computed density lapse rate. The computed first-degree fit for all the data is shown by the straight line drawn through the presented data. The trailing cone in the extended position was 38 feet behind the exhaust pipe of the TV-2 for all tests, both low-level and altitude.

The data shown in Fig. 25 include all those data points whose absolute value of  $\Delta P$  computes to 2.0 pounds per square foot (psf) or less, and the first-degree fit represented by the straight line drawn through the data.

Figure 26 reflects the low-altitude data obtained for the trailing cone system using the Navy F8C pacer. Test Procedures I, II, and III, or a combination of any two of these were used to obtain this information. The method of deriving  $\Delta P$  was similar to that outlined above for the TV-2 at the 200 foot altitude. The trailing cone in its extended position was approximately 63 feet behind the vertical stabilizer of the F8C for all tests.

Figure 27 is similar in form for the F8C as that shown in Fig. 25 for the TV-2. The straight line through the data is representative of the first-degree fit of the data points by linear regression analysis.

The results shown in Fig. 28 are a composite of all validated data obtained at high altitude using the F8C pacer. The Test Procedures used to obtain this data included I, II, or III for the low-level reference velocity points, and IV, V, VI, VII, and VIII or any combination of these procedures for altitude tests.

The method employed to calculate  $\Delta P$  at altitude was that noted in equations (23) and (24). In addition, due to the limitation in available radiosonic data, the computation shown in equation (10) was employed and  $\bar{P}_R$  was assumed to be the accurate representation of  $P_C$  at reference speed.

$$\Delta P = \bar{P}_R - [P_{IT} - P_K \Delta H] \quad (25)$$

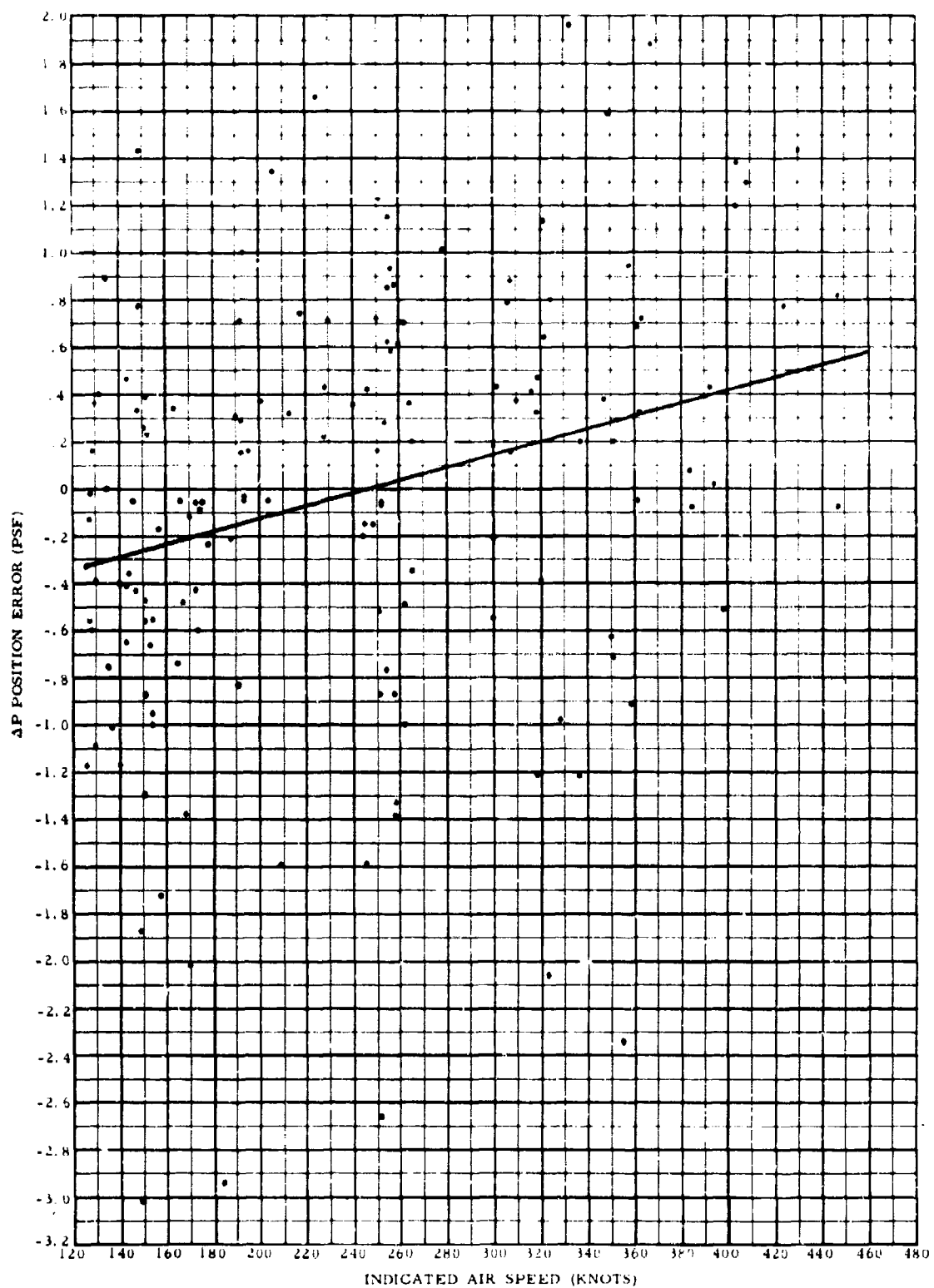


FIG. 24 POSITION ERROR VERSUS INDICATED AIRSPEED -  
TV-2 PACER (LOW ALTITUDE) ALL DATA



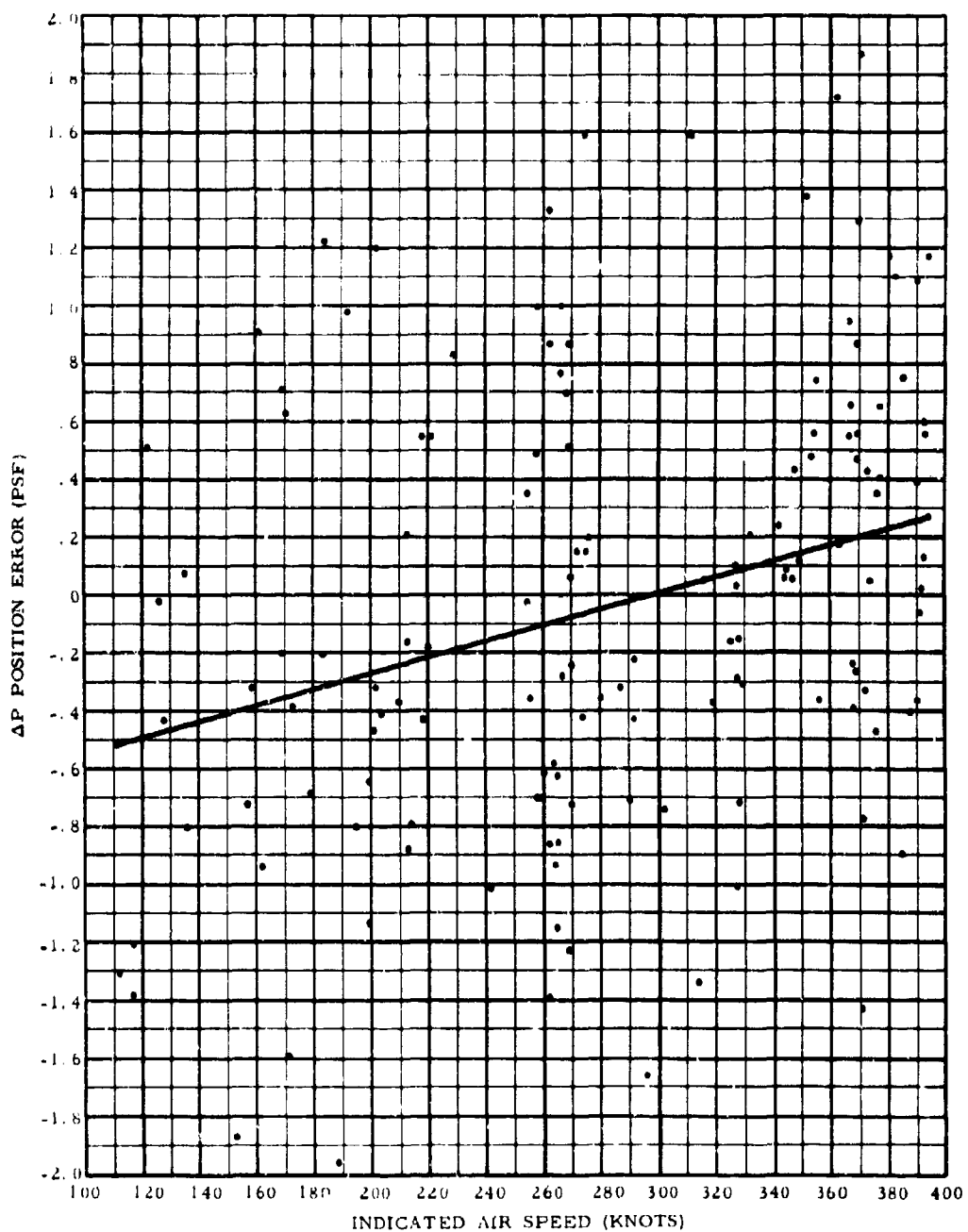


FIG. 25 POSITION ERROR VERSUS INDICATED AIRSPEED -  
TV-2 PACER (LOW ALTITUDE) SELECTED DATA

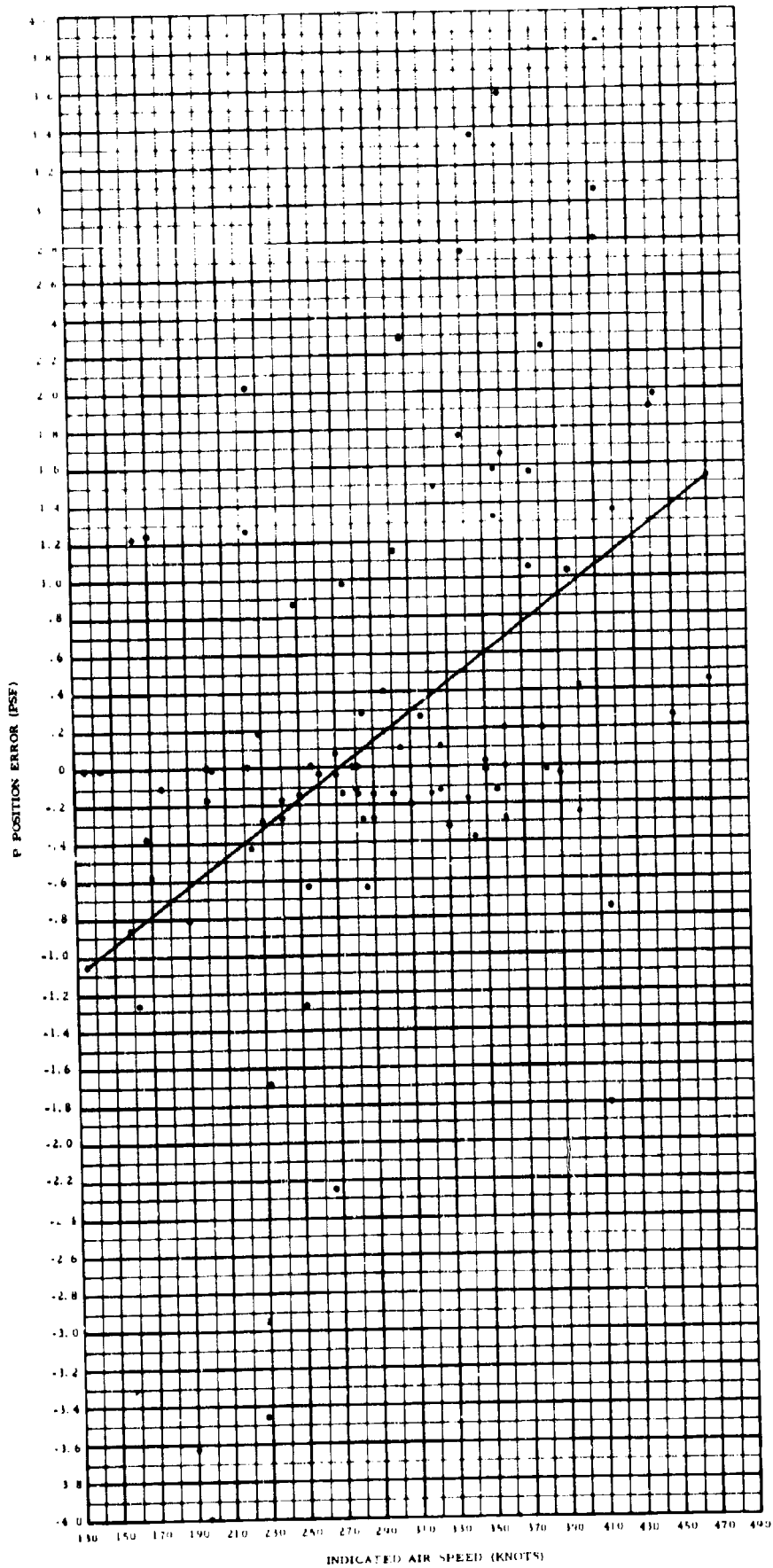


FIG. 26 POSITION ERROR VERSUS INDICATED AIRSPEED -  
F8C PACER (LOW ALTITUDE) ALL DATA

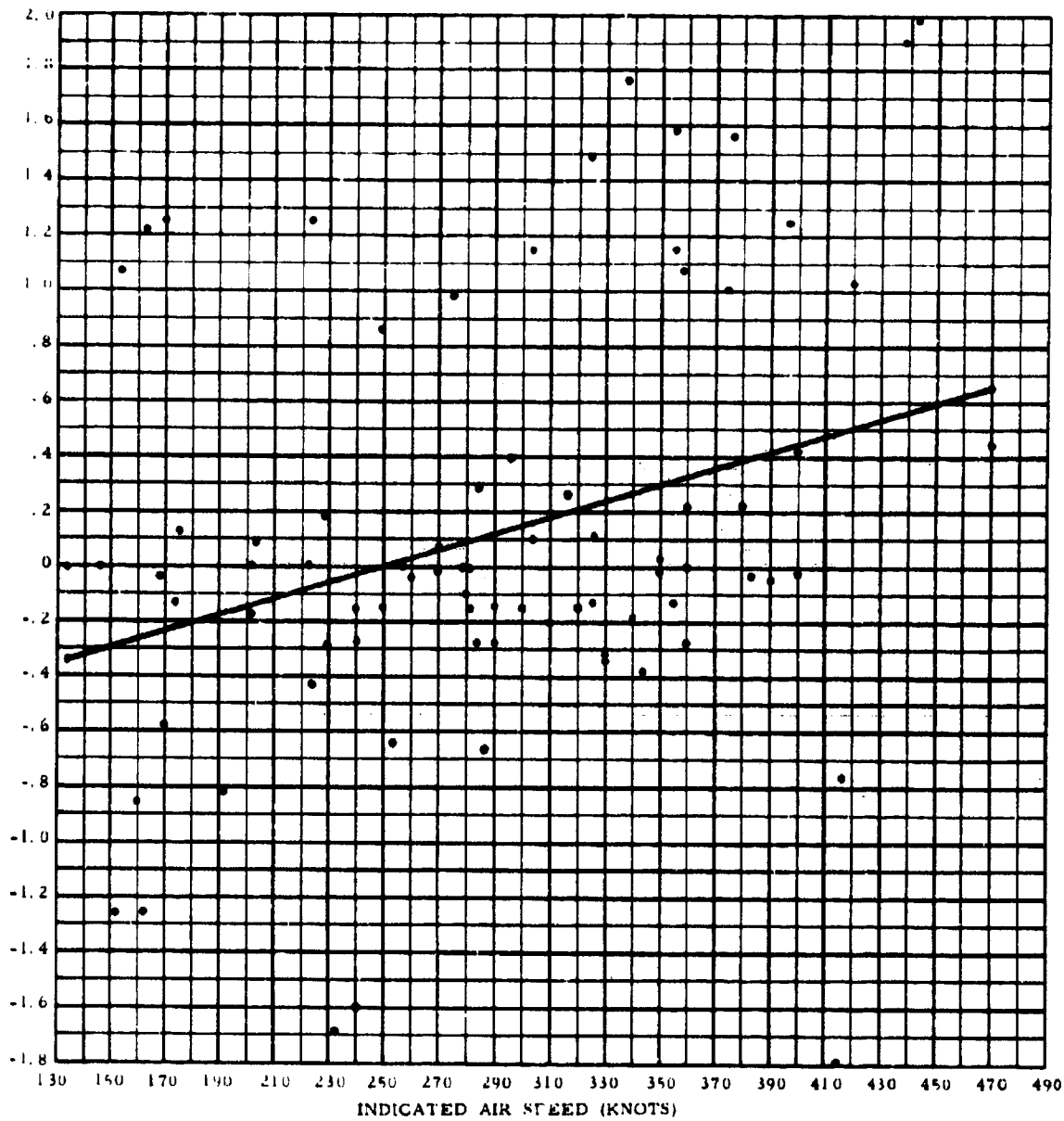


FIG. 27 POSITION ERROR VERSUS INDICATED AIRSPEED -  
F8C PACER (LOW ALTITUDE) SELECTED DATA

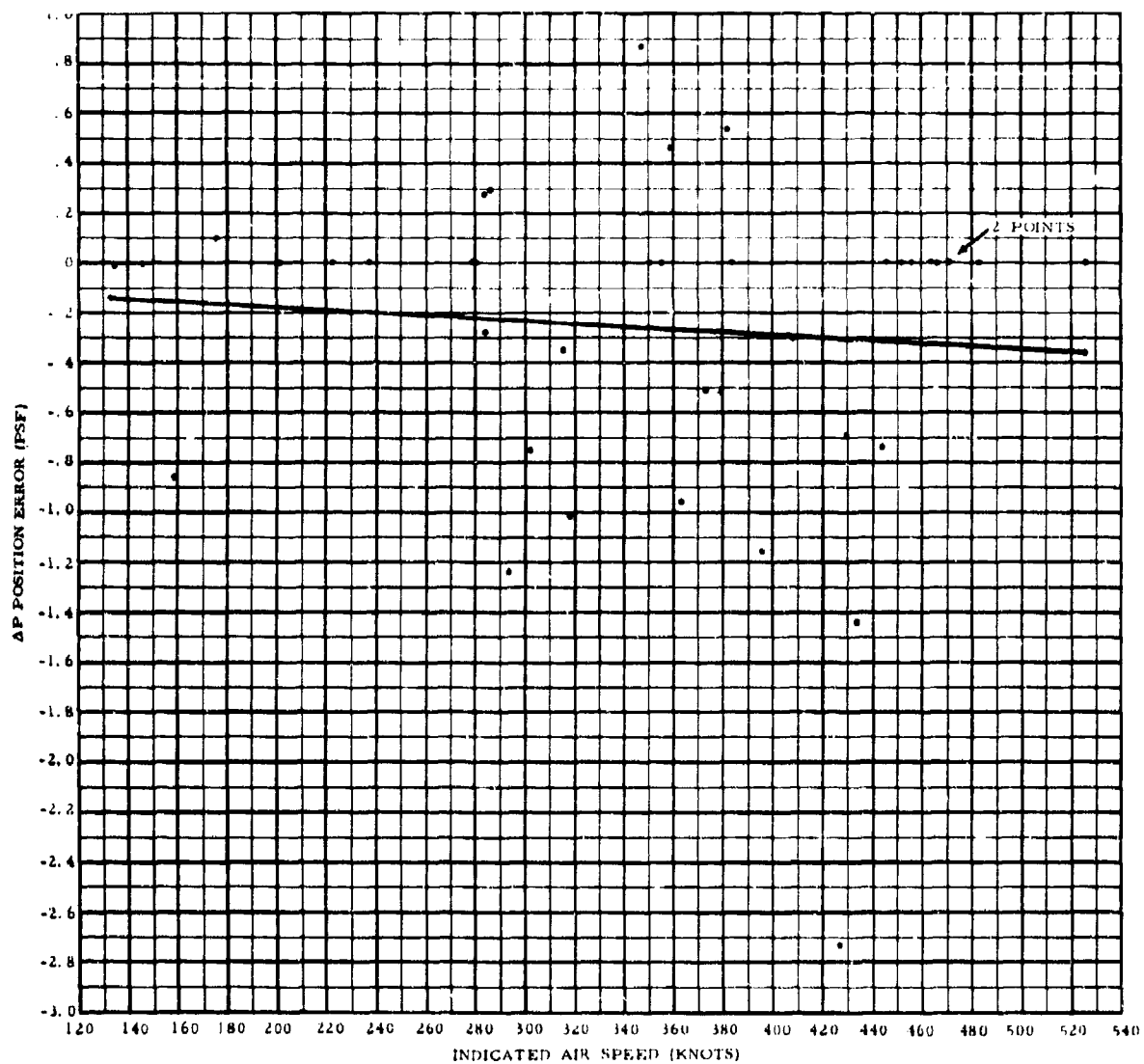


FIG. 28 POSITION ERROR VERSUS INDICATED AIRSPEED -  
F8C PACER (HIGH ALTITUDE) ALL DATA

An additional method of obtaining  $\Delta P$  is to assume the difference between the computed velocity obtained in equations (15) and (17) where available is due to the static pressure error of the airspeed system.

$$\Delta P = f(\bar{V}_1 - [V_{IE} + (V_{CS} - V_{CC})] - \frac{V_{G1} + V_{G2}}{2}) \quad (26)$$

where  $\Delta P$  can be derived from differences in velocity when expressed in terms of dynamic pressure. The values of dynamic pressure can be obtained in terms of  $\Delta P$  from appropriate charts in Reference G.

Figure 29 is a presentation of those data points whose absolute value of  $\Delta P$  computes to 2.0 pounds per square foot or less.

Figure 30 is a composite of all selected data obtained for the trailing cone system at all test altitudes. Approximately 75 percent of the data shown exhibits a  $\Delta P$  of less than  $\pm 1.0$  psf. This is equal to approximately  $\pm 12$  feet or less at sea level, and  $\pm 30$  feet or less at 30,000 feet. These absolute values of  $\Delta P$  are within the overall accuracy of each of the several systems involved in the measurement of the various parameters.

Figures 31 through 34, inclusive, reflect the position error as a function of dynamic pressure and Mach Number. This presentation is the more common technical representation of the static pressure defect.

Figure 35 depicts the statistically-derived position error in terms of feet. Shown are the curves for both sea level and 30,000 feet based on a model atmosphere. Also shown are the respective variations of 75 percent of the observed data which was approximately  $\pm 12$  feet at sea level, and  $\pm 30$  feet at 30,000 feet.

The test results shown in Figs. 24 through 35 are based on aircraft performance with the aircraft in steady-state unaccelerated level flight with no control surface movement or power changes. It was noted during the data gathering and testing that aircraft acceleration, or surface control movement at a time when data was being taken, had adverse effects on the data.

FIG. 30 POSITION ERROR VERSUS INDICATED AIRSPEED -  
ALL DATA

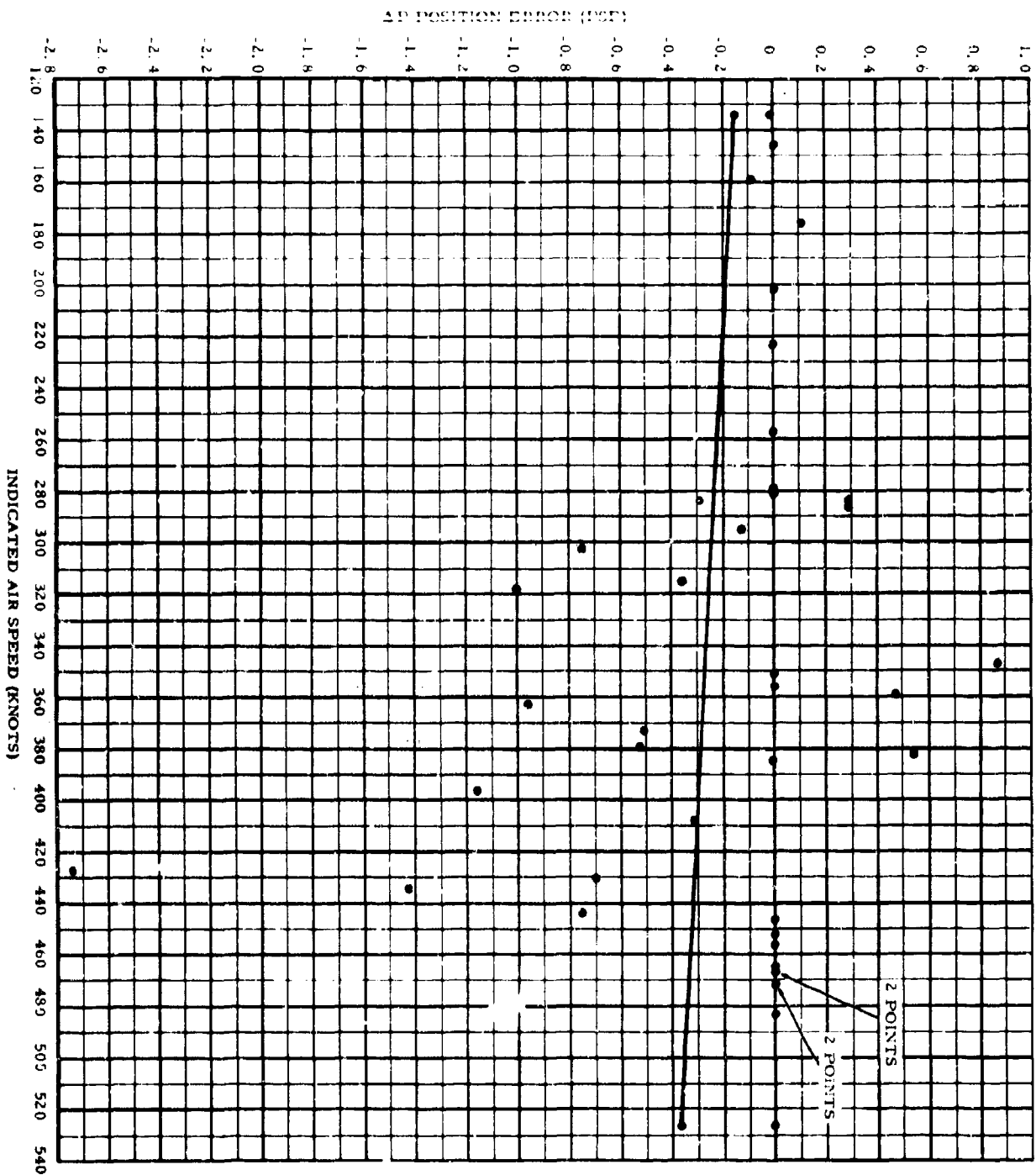


FIG. 29 POSITION ERROR VERSUS INDICATED AIRSPEED -  
F8C PACER (HIGH ALTITUDE) SELECTED DATA

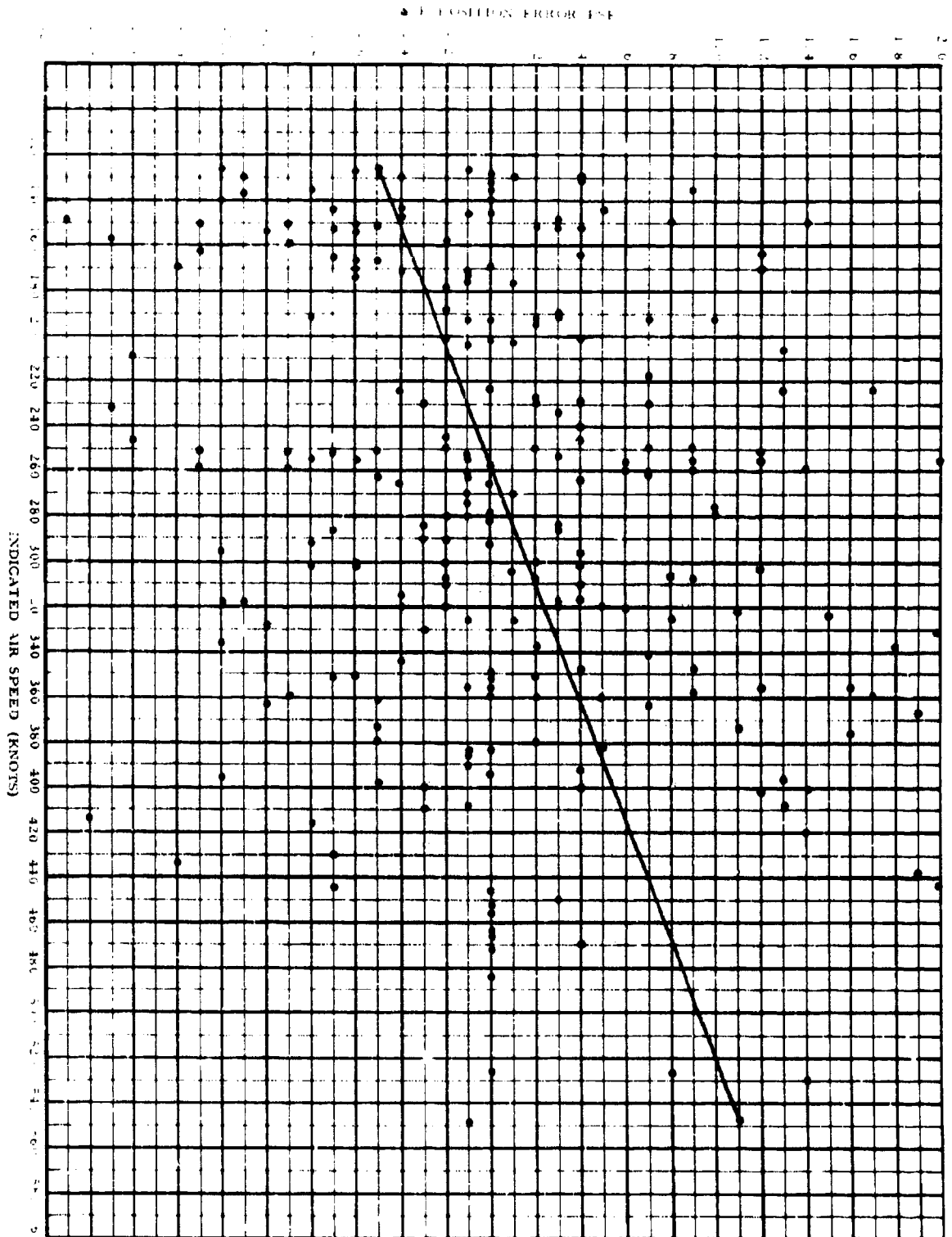


FIG. 30 POSITION ERROR VERSUS INDICATED AIRSPEED -  
ALL DATA

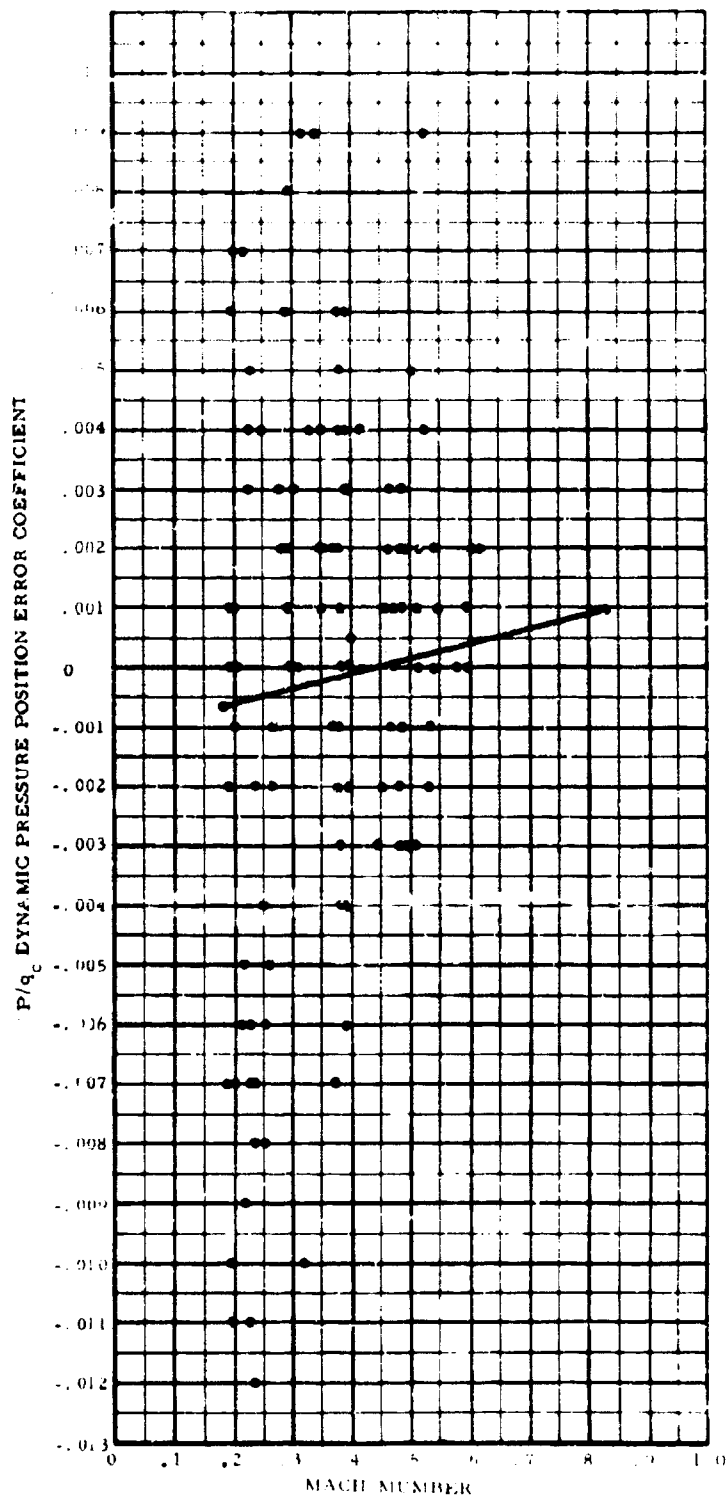


FIG. 31  $\Delta P/q_c$  VERSUS Mn TV-2 PACER



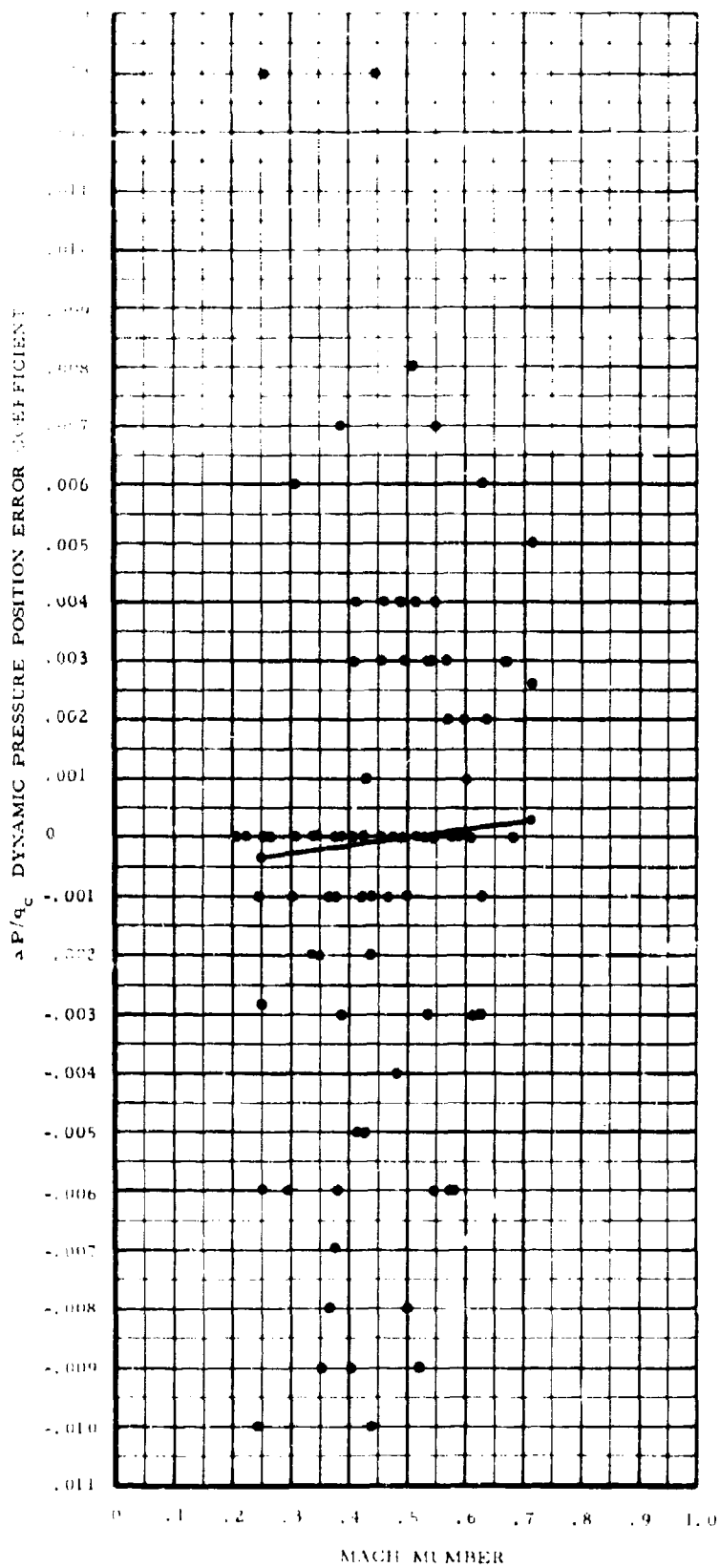


FIG. 32  $\Delta P/q_c$  VERSUS  $M_n$  F8C LOW ALTITUDE

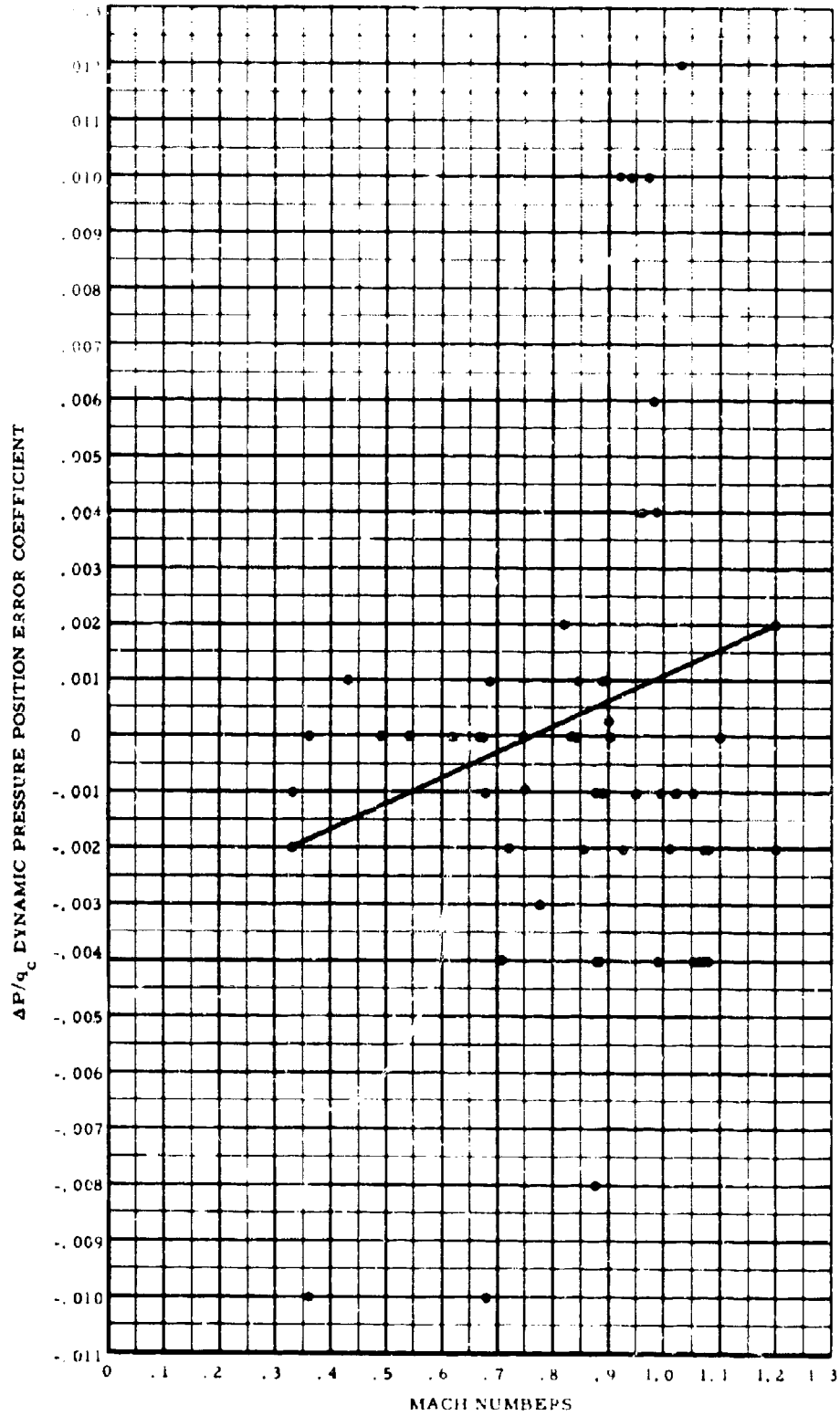


FIG. 33  $\Delta P/q_c$  VERSUS  $M_n$  F8C HIGH ALTITUDE

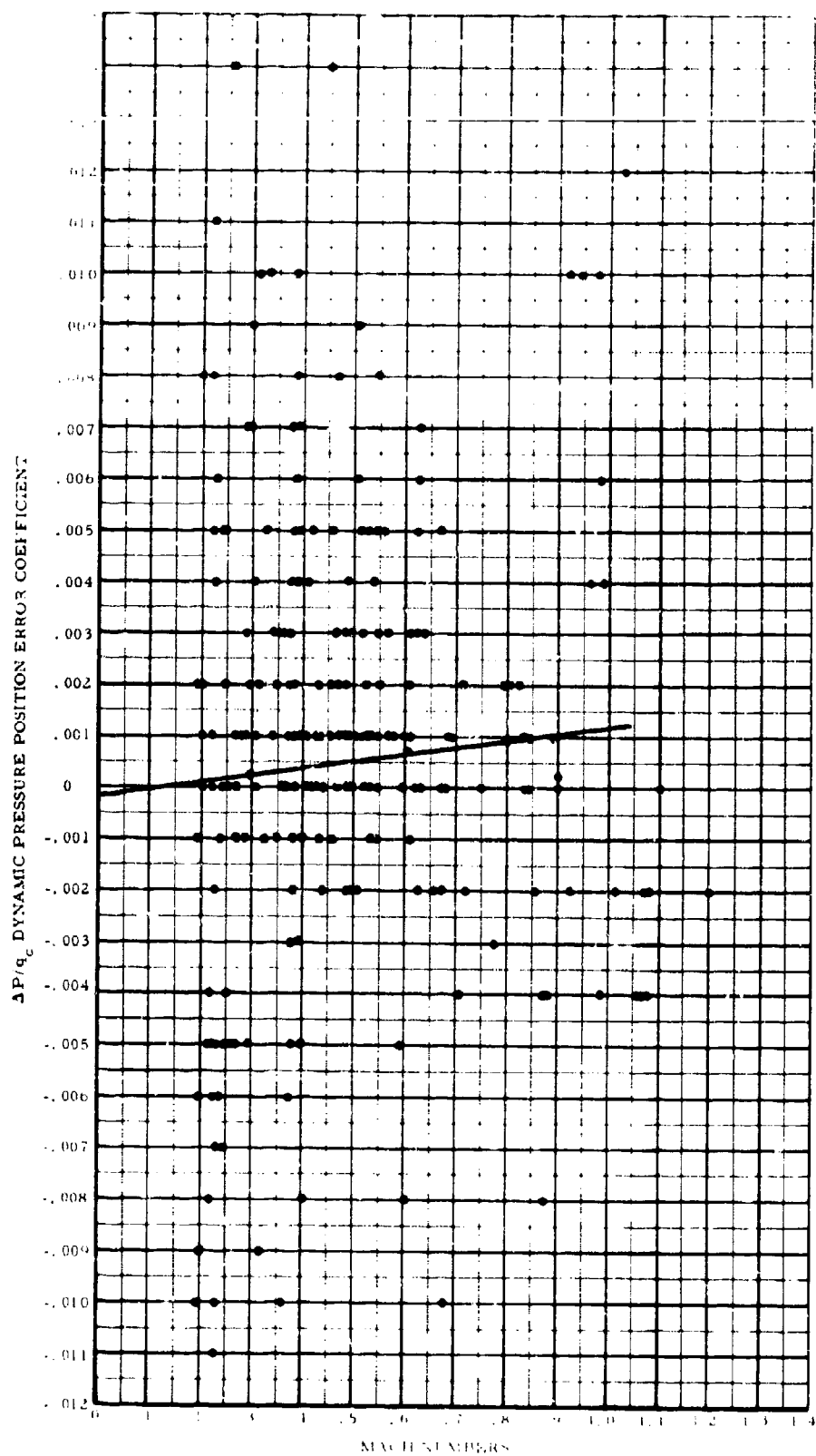
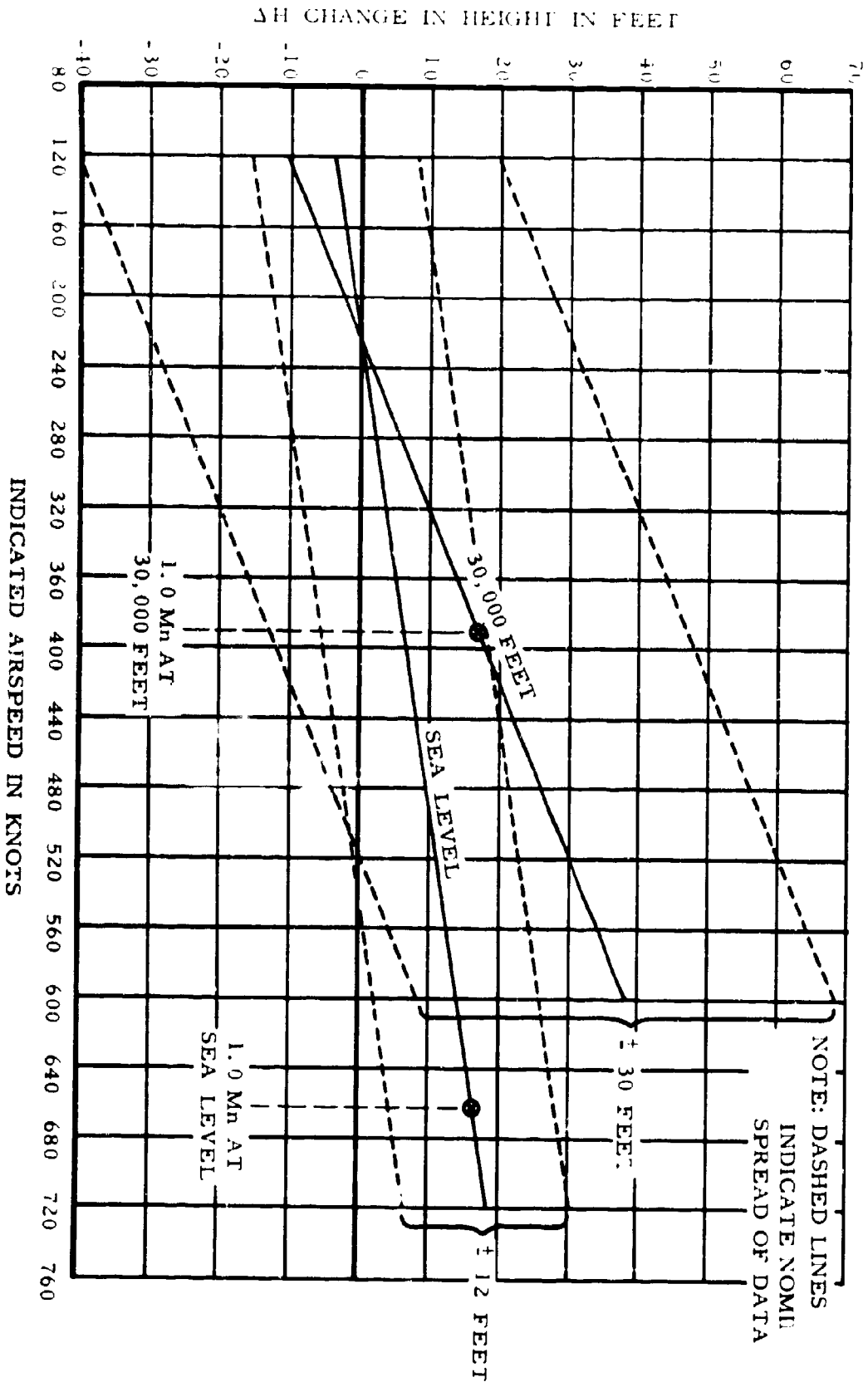


FIG. 34  $\Delta P/q_c$  VERSUS  $M_n$  ALL DATA

FIG. 35  $\Delta H$  VERSUS IAS ALL DATA

## CONCLUSIONS

Based on the test results shown, the following conclusions may be drawn:

1. The trailing cone system does not exhibit any significant error as a function of the towing aircraft when the aircraft is flown in unaccelerated, level flight (Figs. 25 and 27).
2. The system does not exhibit any noticeable Mach effect up to 1.12 Mn (Fig. 34).
3. Due to the basic design, the system does not have a measurable angle-of-attack sensitivity.

Based on observed flight performance and pilot comments, the following is concluded:

1. The system does not interfere with nor affect the controllability of the towing aircraft.
2. The use of the system as a component of the airspeed system gives a satisfactory instrument presentation without the non readable oscillatory behavior normally encountered when accelerating through Mach 1.0.

## RECOMMENDATIONS

It is recommended that the trailing cone system be employed as a standard to determine the position error of the static pressure portion of an aircraft's airspeed system. Position error determination using this method must be accomplished when the aircraft is in unaccelerated level flight.

# LIST OF SYMBOLS

- $D$  = Drag.
- $g$  = Local gravity.
- $\Delta H$  = Difference in geometric height of station elevation and test altitude.
- $\Delta h$  = Difference in elevation between observed ground reading and station elevation.
- $N$  = Number of observations relating to a given defined grouping.
- $N'$  = Number of observations relating to a given defined grouping other than that used for  $N$ .
- $\Delta P$  = Position error.
- $P_B$  = Preflight calibration bias.
- $P_{BC}$  = Observed corrected barometric pressure of the base of a given air column.
- $P_{BC}'$  = Observed corrected barometric pressure at some known point in a given air column.
- $P_{BCN}$  = Observed corrected barometric pressure closest to the test altitude.
- $P_C$  = Computed pressure at test altitude.
- $\Delta P_C$  = Change in computed station pressure due to  $\Delta H$ .
- $P_G$  = Known ground station pressure.
- $\bar{P}_{GC}$  = Mean computed ground station pressure.
- $P_{GI}$  = Indicated ground station pressure.
- $P_{GP}$  = Calibration correction term of scale for a given value of  $P_{IT}$ .
- $P_{GT}$  = Calibration correction factor due to ambient temperature of the barometer.
- $P_{IC}$  = Calibrated local pressure.
- $\Delta P_{IC}$  = Change in calibrated local pressure.
- $\bar{\Delta P}_{IC}$  = Mean change in calibrated local pressure between reference test speeds.
- $P_{IR}$  = Indicated local pressure at a given reference speed.
- $P_{IT}$  = Indicated local pressure.
- $P_K$  = Rate of change in pressure at station elevation based on a model atmosphere.
- $\bar{P}_{KC}$  = Mean computed pressure lapse rate.
- $P_R$  = Corrected reference pressure based on horizontal pressure survey preceding test.
- $\bar{P}_R$  = Mean ambient reference pressure.
- $P_R'$  = Corrected reference pressure based on horizontal pressure survey following test.
- $P_S$  = Standard day pressure at station elevation.
- $q_c$  = Dynamic calibrated pressure.
- $R$  = Gas constant for dry air.
- $T_C$  = Computed temperature at test altitude based on vertical profile of air column temperature.
- $\bar{T}_{GC}$  = Mean ground station temperature.

LIST OF SYMBOLS (continued)

$T_s$  = Standard dry air temperature at station elevation.  
 $V$  = Calibrated velocity of aircraft.  
 $V_C$  = Calibrated airspeed.  
 $V_{CC}$  = Calibrated airspeed from trailing cone indication.  
 $V_{CS}$  = Calibrated airspeed from aircraft system indication.  
 $V_{G1}$  = Tracked ground speed in direction A.  
 $V_{G2}$  = Tracked ground speed in direction A + 180°.  
 $V_I$  = Indicated airspeed.  
 $V_{IE}$  = Scale error of Indicator.  
 $W$  = Weight in pounds.  
 $\alpha$  = Angle of attack.  
 $\rho_c$  = Computed local density of air mass.  
 $\rho_{GC}$  = Computed density at the base of the air column.  
 $\rho_s$  = Model atmospheric density for a given elevation.

## REFERENCES

- A    Anonymous, Accuracies of Radiosonde Data. U.S.A.F. (MATS)  
Tech. Report 105-133.
- B    Anonymous, Memorandum on Density Altitude, U.S.A.F. (A.W.S.)  
Tech. Report TR 105-101.
- C    Anonymous, Optical Tracker Evaluation and Accuracy Test System,  
U.S. Army (Sig Corps) ASTIA 270638.
- D    Anonymous, Radiosonde Observation Computation Tables and  
Diagrams, U.S.A.F. (A.W.S.) Tech. Report 105-64.
- E    Anonymous, Empirical Frequency Distribution of Pressure,  
Temperature and Air Density at Levels of Constant Altitude,  
U.S. Army (Missile Command) TR 61-28.
- F    Anonymous, SRDS Technical Facilities, RD P 6000.2.
- G    Bartlett, E. P., Performance Flight Test Handbook, U.S.A.F.  
AFFTC-TN-29-22.
- H    Butler, C. M. and Haller, N. M., An Investigation of the  
Feasibility of Indicating Altitude by Gravimetric Measurements,  
ASTIA 278112.
- I    Deleo, R. V. and Hagen, F. W., Evaluation of New Methods for  
Flight Calibration of Aircraft Instrument Systems, U.S.A.F.  
(WADC) TR 59-295.
- J    Fine, R. L., Flight Test Evaluation of Aircraft Pressure  
Altimeter Installations, U.S.A.F. (WADC) TN 56-438.
- K    Flickinger, H. S., Test and Data Reduction Procedures for  
Static Pressure Position Error Calibration by Altimeter-  
Depression Methods, U.S. Navy (NATC) TM 4-53.
- L    Gracey, W., Measurement of Static Pressure on Aircraft,  
NACA Report 1364.
- M    Gracey, W., Measurement of Static Pressure on Aircraft,  
NACA RM L57A09.
- N    Gracey, W., Position Errors of the Service Airspeed  
Installations of 10 Airplanes, NACA TN 1892.



# REFERENCES (continued)

- O Gracey, W., Measurement of Static Pressure on Aircraft.  
NACA TN 4184.
- P Gracey, W. and Shipp, J. A., Random Deviations from Cruise Altitudes of a Turbojet Transport at Altitudes Between 20,000 and 41,000 feet, NASA TN D-320.
- Q Hanks, N. J., Altitude Separation Program, U.S.A.F. TM-56-28.
- R Hesse, W. J., Position Error Determinations by Stadiametric Ranging, U.S. Navy (NATC) TR 2-55.
- S Holbeche, T. A., and Spence, D. A., Temperature Measurements Behind an Attenuating Shock Wave, R.A.E. Aero 2883.
- T Horkey, E. J., A Method of Airspeed Calibration at High Mach Numbers Without Reference to the Ground, North American Aviation Report NA-49-775.
- U James, P., Lindsay, J. L., Trant, Jr. and Zalovecik, J. A., A Method of Calibrating Airspeed Installations on Airplanes at Transonic and Supersonic Speeds by the Use of Accelerometer and Attitude-Angle Measurements, NACA Report 1145.
- V Knowler, A. E., Lock, C. N. H. and Pearcey, H. H., The Effect of Compressibility on Static Heads, ARC Report 2386.
- W Martin, T. A. and White, W. E., Transonic Investigation of Three Pitot-Static Probes Designed for Pressure-Error Compensation, U.S.A.F. (AEDC) 62-123.
- X Piccard, J., Proceedings of Altimetry Conference, FAA, Bureau of Research and Development, March 31, 1960.
- Y Price, E. N., A System for Providing and Measuring Free Stream Static Pressure, Douglas Aircraft Co. DEV 3519.
- Z Richardson, N. N., Forecasting Density Altitude, U.S.A.F. (MATS) Tech. Report 165.
- AA Ritchie, V. S., Several Methods for Aerodynamic Reduction of Static Pressure Sensing Errors for Aircraft at Subsonic, Near-Sonic, and Low Supersonic Speeds, NASA TR R-18.

REFERENCES (continued)

- AR Shrager, J. J., Survey of Altimeter Instrument and Position-Error for CAR 3 Type Aircraft, FAA SRDS Report 115-22D.
- AC Shrager, J. J., Calibrating Static Pressure Systems at Low Altitude, FAA(SRDS) RD 64-37.
- AD Siegel, R. B., Acceleration - Deceleration Method of Calibration of the Static Pressure Position Error in the Transonic Flight Region, U. S. Navy (NATC) TM 1-60.
- AE Smetana, F. O., Stuart, J. W., and Wilber, F. C., Investigation of Free Stream Pressure and Stagnation Pressure Measurement from Transonic and Supersonic Aircraft, U.S.A.F. (WADC) 55-238.
- AF Smith, A. F., Digital Optical Tracking System, U.S.A.F. (ASD) TR-61-358.
- AG Smith, K., Pressure Lag in Pipes, R.A.E. Report Aero 2507.
- AH Smith, K. W., The Measurement of Position Error at High Speeds and Altitude by Means of a Trailing Static Head, A.R.C. 160.
- AI Werner, F. D. and Geronime, R. L., Automatic Correction of Errors in Airplane Static Pressure Sources, U.S.A.F. (WADC) 56-193.
- AJ Wright, W. F., A Survey for Naval Ordnance Laboratory of High Altitude Atmospheric Temperature Sensors and Associated Problems, ASTIA 278152.
- AK Zalovcik, J. A., A Radar Method of Calibrating Airspeed Installations on Airplanes in Maneuvers at High Altitudes and at Transonic and Supersonic Speeds, NACA Report 985.

<p>UNCLASSIFIED</p> <p>I. Sreager, Jack J. II. Project No. 320-205-02X III. Report No. RD-GA-156</p> <p>Descriptives</p> <p>Altitude Air Transportation Civil Aviation Airspeed Airworthiness Aviation Safety</p> <p>UNCLASSIFIED</p>	<p>UNCLASSIFIED</p> <p>I. Sreager, Jack J. II. Project No. 320-205-02X III. Report No. RD-GA-156</p> <p>Descriptives</p> <p>Altitude Air Transportation Civil Aviation Airspeed Airworthiness Aviation Safety</p> <p>UNCLASSIFIED</p>	<p>UNCLASSIFIED</p> <p>I. Sreager, Jack J. II. Project No. 320-205-02X III. Report No. RD-GA-156</p> <p>Descriptives</p> <p>Altitude Air Transportation Civil Aviation Airspeed Airworthiness Aviation Safety</p> <p>UNCLASSIFIED</p>	<p>UNCLASSIFIED</p> <p>I. Sreager, Jack J. II. Project No. 320-205-02X III. Report No. RD-GA-156</p> <p>Descriptives</p> <p>Altitude Air Transportation Civil Aviation Airspeed Airworthiness Aviation Safety</p> <p>UNCLASSIFIED</p>
<p>UNCLASSIFIED</p> <p>I. Sreager, Jack J. II. Project No. 320-205-02X III. Report No. RD-GA-156</p> <p>Descriptives</p> <p>Altitude Air Transportation Civil Aviation Airspeed Airworthiness Aviation Safety</p> <p>UNCLASSIFIED</p>	<p>UNCLASSIFIED</p> <p>I. Sreager, Jack J. II. Project No. 320-205-02X III. Report No. RD-GA-156</p> <p>Descriptives</p> <p>Altitude Air Transportation Civil Aviation Airspeed Airworthiness Aviation Safety</p> <p>UNCLASSIFIED</p>	<p>UNCLASSIFIED</p> <p>I. Sreager, Jack J. II. Project No. 320-205-02X III. Report No. RD-GA-156</p> <p>Descriptives</p> <p>Altitude Air Transportation Civil Aviation Airspeed Airworthiness Aviation Safety</p> <p>UNCLASSIFIED</p>	<p>UNCLASSIFIED</p> <p>I. Sreager, Jack J. II. Project No. 320-205-02X III. Report No. RD-GA-156</p> <p>Descriptives</p> <p>Altitude Air Transportation Civil Aviation Airspeed Airworthiness Aviation Safety</p> <p>UNCLASSIFIED</p>